NEURAL MECHANISMS FOR SPECTRAL ANALYSIS IN THE AUDITORY MIDBRAIN, THALAMUS, AND CORTEX

Monty A. Escabí* and Heather L. Read†

*Department of Electrical Engineering, University of Connecticut
Storrs, Connecticut 06269, USA
†Department of Psychology, The University of Connecticut, Storrs, Connecticut 06269, USA

Frequency organization or cochleotopy is a fundamental aspect of the lemniscal "high fidelity" auditory system. Starting with the cochlear sensory epithelium, a systematic gradient of frequency-tuned neuronal receptors can be observed at all levels of the central auditory system. Distinct spectral processing pathways with unique monaural integration response properties are initially set up in the cochlear

INTERNATIONAL REVIEW OF NEUROBIOLOGY, VOL. 70
DOI: 10.1016/S0074-7742(05)70007-6

0074-7742/05 $35.00

nucleus (CN), and subsequently refined into binaural processing streams in the superior olivary nuclei (SO). At the level of the auditory midbrain and beyond these separate sources of frequency-specific binaural/monaural input intermingle with one another giving rise to new types of modularity and cochleotopy. Here we examine the anatomical organization of neuronal response preferences in the auditory midbrain, thalamaus, and cortex within a framework of functional modularity and bottom up intrinsic connectivity. Spectral preferences are intimately related to the type of binaural preference and sound level dependence and yet we know very little about their basic organization within these centers. An emphasis is placed on reconciling neuronal, anatomic, and physiologic principles underlying spectral analysis and perceptual phenomena, in particular, frequency resolution, loudness perception, and sound localization.

I. Introduction

This chapter examines the principles of spectral analysis and coding in the ascending central auditory system. The chapter is centered around identifying key response properties of single neurons in the lemniscal divisions of the inferior colliculus (ICC), auditory thalamus (MGBv), and primary auditory cortex (AI) that can be related to the underlying anatomical architecture in these stations. Starting with the divergent pathway from the cochlea to the brainstem nuclei, the ICC receives input from the cochlear nucleus (CN), superior olivary nuclei (SO), and the nucleus of the lateral lemniscus (NLL) (Adams, 1979). This highly convergent pattern of innervating input from multiple brainstem nuclei plays a key role in refining the organization of spectral and temporal preferences in the ICC. Within this context, spectral and temporal preferences in the ICC are sequentially modified in the thalamus and cortex leading to distinct differences in the functional organization. This functional and anatomical framework is essential for understanding the distributed code for spectral and temporal features in a sound.

The chapter emphasizes the general principles of coding which serve as a functional and anatomical substrate for spectral analysis in the central auditory system. In particular, we focus on relating details of single neuron activity to the underlying anatomical layout and connectivity at different levels of the lemniscal auditory pathway. Spectral response properties and selectivity are intimately related to binaural preferences and sound level dependence. Throughout we explore the specific relationships between these different response attributes and the underlying local circuitry and global organization of the central auditory system. General properties of single neuron sensitivities are outlined in Sections II to V whereas their relationship to the anatomical circuitry and the underlying functional transformation is described in Sections VI to VIII.

II. Principles of Spectral Analysis in ICC, MGB, and AI

The frequency organization of the cochlear sensory epithelium is conserved in the topographic pattern of neuronal frequency selectivities or cochleotopy. A cochleotopic pattern of frequency response properties is observed throughout the lemniscal auditory pathway including the ICC, MGBv, and AI. Demonstrating the functional consequences associated with specific anatomical patterns of frequency specific projections in the lemniscal pathway requires efficient and meaningful ways of characterizing spectral sensitivities. The receptive field (RF) is the classical method of measuring and quantifying neuronal sensitivities.

Auditory RFs are defined by the rate or time-locked responses of neurons to sound structure including spectral content or frequency, sound level, and modulation rate. Spectral receptive field (SRF) preferences are usually obtained by measuring the response to various simple acoustic parameters, such as frequency and amplitude, as is done when measuring frequency tuning curves (FTCs) or frequency response areas (FRAs). Figure 1 illustrates two AI neuron FTCs generated by varying the frequency and sound pressure level (SPL) of the same transient pure-tone presented to both ears. This is the classic method for determining simple spectral selectivities for auditory neurons; however, many spectral RF properties cannot be assessed with such narrow bandwidth sounds. As will be seen, the measured characteristics of an SRF depend dramatically on a number of factors, such as the type of stimulus used (e.g., broadband versus narrowband), its sound level, dynamic range or contrast, and even the temporal attributes of the sound. Such non-linear properties of the sound sensitivity of collicular, thalamic, and cortical receptive fields make it difficult to relate neuronal activities of one sound to another and present an interpretational challenge in the study of central auditory system function.

III. Sharpness of Tuning, Bandwidth, and Level Dependence

Frequency and absolute sound level are important attributes in complex sounds that are known to influence perception. The spectrum of communication sounds and other behaviorally relevant environmental signals can vary significantly in their frequency content and amplitude level. Frequency content, disparity in frequency composition for the two ears, and absolute sound level can also encode for the location of sound sources. It is the task of the central auditory system to faithfully represent the sound so that different sounds can be discriminated. At the same time, the system must disambiguate frequency and loudness differences that are due to differences in sound location. The first step to

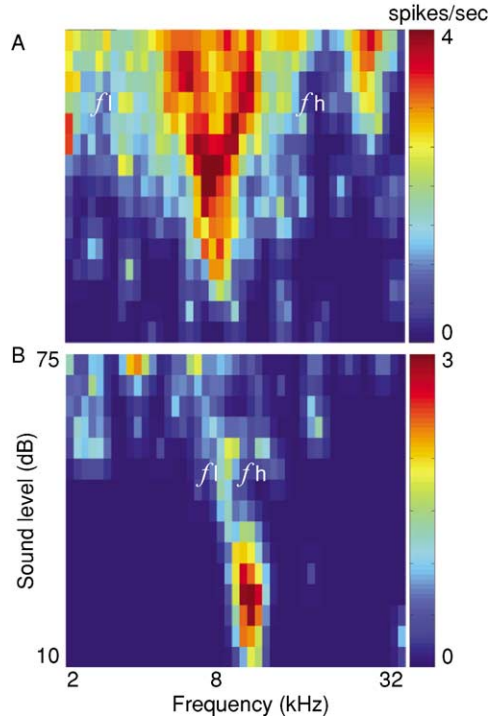

FIG. 1. Two cortical FTCs for pure tone sounds. Tone frequency and amplitude are varied over 5 octaves and 70 dB, respectively. Multi- or single-unit neuronal spike rate histograms are plotted for each frequency and level. The rainbow color spectrum shows lowest to highest spike rates (blue to red). Threshold is the lowest sound level eliciting a response above baseline. Characteristic frequency (CF) is the frequency at threshold. Linear bandwidth is the difference between the high (fh) and lower (fl) cutoff frequency at a given sound level. Examples A and B are broad bandwidth and narrow bandwidth FTCs, respectively. The rate level functions increase monotonically and non-monotonically with sound level for A and B, respectively. Neurons with non-monotonic narrow bandwidth FTCs in cortex are likely azimuth tuned (Clarey *et al.*, 1995; Barone *et al.*, 1996).

understanding how populations of neurons represent frequency content, loudness, and location of sounds is to develop reliable ways of characterizing the responses of individual neurons to these sound cues.

Neurons can be coarsely defined as having either monotonic or non-monotonic sound level dependence for spike rate. Changing the sound level has systematic effects on the response spike rate, temporal precision, and response latency. Monotonic rate-level coding can be demonstrated with a variety of narrowband and broadband sounds. Firing rates increase monotonically with

increasing sound level for a large proportion of central auditory neurons (Ehret and Merzenich, 1988a; Heil, 1997c; Heil *et al.*, 1994; Phillips and Irvine, 1981; Phillips *et al.*, 1985; Rees and Palmer, 1988; Rose *et al.*, 1963; Rouiller *et al.*, 1983; Schreiner *et al.*, 1992; Semple and Kitzes, 1985). At the same time, the response latency is reduced and the timing precision improved with increased sound level (Heil, 1997a). While this type of monotonic rate-level coding is characteristic of the auditory nerve (AN) (Evans and Palmer, 1980), coding of sound level in central stations is distinguished by the fact that a significant fraction of neurons are also inhibited by loud sound levels (Ehret and Merzenich, 1988a; Heil *et al.*, 1994; Phillips and Irvine, 1981; Phillips *et al.*, 1985; Rees and Palmer, 1988; Rose *et al.*, 1963; Rouiller *et al.*, 1983; Schreiner *et al.*, 1992). The firing rate of such neurons initially increases with SPL and is subsequently reduced at a very loud SPL, exhibiting a non-monotonic rate-level dependency.

There are generally two conceptual models explaining the distribution of non-monotonic versus monotonic rate level functions between ICC and cortical stations of processing. According to the first, the proportion of non-monotonic responses increases from the ICC to AI (Phillips and Irvine, 1981; Rees and Palmer, 1988; Rouiller *et al.*, 1983; Schreiner *et al.*, 1992), consistent with an increased recruitment of inhibition across this pathway. According to the second model, robust non-monotonic rate-level sensitivities are established early on in CN, in particular within the DCN, and conserved at the level of ICC, MGBv, and AI (Barone *et al.*, 1996; Cant and Benson, 2003; Davis and Young, 2000; Ramachandran *et al.*, 1999). The subtle distinction between these two models is that the first suggests novel inhibitory processes at each level which refine rate-level sensitivities whereas the second suggests that there are "parallel auditory pathways" originating in the CN that pass on and conserve the different rate-level sensitivities observed in ICC, MGBv, and AI (Cant and Benson, 2003). Indeed, the non-monotonic rate level functions observed in the DCN are very similar to those observed for a subset of neurons in the MGBv and AI (Barone *et al.*, 1996). Non-monotonic rate-level dependence could also be created or maintained via ascending inhibitory projections from the sub-collicular nuclei to the colliculus (Oliver and Shneiderman, 1989; Shneiderman and Oliver, 1989; Shneiderman *et al.*, 1988) and again from the colliculus to the MGBv (Peruzzi *et al.*, 1997; Winer *et al.*, 1996). Local inhibitory neurons at each level of processing also could contribute to the level dependence and other SRF properties at each station of the pathway, including early stages such as the CN. Direct correlations between sources of inhibitory input and sound level dependency have been described in the cat DCN (Davis and Young, 2000) and in the bat ICC (Pollak and Park, 1993) but not in the MGBv or AI. Hence, at present both models for how non-monotonic level dependencies are modified centrally are still plausible.

Sound-level-dependent firing rates (monotonicity versus non-monotonicity) and bandwidths often co-vary and these two parameters are derived from the pure-tone FTC or frequency response areas (FRAs). The exact shape of the FRA depends on a number of factors, including the tone-pip duration, rise time, and the time window used to acquire spike activity. FRAs in the ICC, MGBv, and AI typically only account for the excitatory component of the neuronal response. These can vary in their structure from narrowband to broadband excitatory sensitivity and can vary in their shape from simple eighth nerve-like FRA response sensitivity to more intricate FRA shapes (Ehret *et al.*, 2003; Stiebler and Ehret, 1985; Sutter and Schreiner, 1991). Example broadband and narrowband FRAs from cat AI are illustrated in Fig. 1. Because of this diversity in excitatory FRA shapes, FRAs have been categorized according to a number of functional parameters that account for the spectral filtering preferences. These include the frequency with maximal response (best frequency BF), the frequency with the lowest response threshold (characteristic frequency CF), and the sharpness of tuning measured as either a bandwidth in units of octaves or the quality factor (Q, defined as the ratio of CF to bandwidth). A decreased spectral resolution at loud sound levels is observed for all sensory fibers in the cochlea, whereas the filter resolution of ICC, MGBv, and AI neurons and their corresponding level dependence are more heterogeneous (Barone *et al.*, 1996; Langner and Schreiner, 1988; Phillips and Irvine, 1981; Schreiner and Mendelson, 1990).

The type of sound level response dependence is also closely related to other receptive field properties including the spectral sensitivity. In the ICC of decerebrate cats, for instance, monotonic responses have characteristic V-shaped frequency response areas as observed for all VIII AN fibers (Evans and Palmer, 1980). Non-monotonic rate-level response functions, however, are strictly observed for neurons with type I and type O frequency sensitivity (Ramachandran *et al.*, 1999) (see Chapter 7). For thalamic and cortical neurons, sound level-dependent changes in spectral bandwidth also appear to correlate with sound level-dependent changes in firing rate. In the cat, monotonic neurons are often characterized by V-shaped FRAs in which the bandwidth increases with level (Phillips *et al.*, 1985; Schreiner *et al.*, 1992). Neurons with type V-shaped FRAs respond efficiently to both narrowband tones and broadband stimuli (e.g., clicks and noise) and have short latency responses to tones and noise (Phillips *et al.*, 1985). By comparison, non-monotonic neurons often exhibit FRAs with narrowband tuning, typically have longer response latencies, and are inhibited by broadband noise bursts and clicks (Phillips *et al.*, 1985; Ramachandran *et al.*, 2000). Non-monotonic rate level dependence can be demonstrated with either pure-tones or broadband sounds. On the other hand, receptive field properties such as azimuth tuning of non-monotonic neurons can only be observed with broadband sounds (Barone *et al.*, 1996). This dissociation between rate and

spectral bandwidth dependence on sound level tuning may be indicative of more than one inhibitory or adaptive mechanism.

IV. Excitatory and Inhibitory Receptive Field Properties

Inhibitory processes are initially established early on in the CN (Davis and Young, 2000), and further refined at more central centers. Feed-forward inhibitory projections from multiple auditory centers play a prominent role in shaping spectral sensitivities. This receptive field shaping could occur via long range tonotopically organized inhibitory projections from the dorsal nucleus of the lateral lemniscus (DNLL) to the ICC (Bajo *et al.*, 1999; Oliver and Shneiderman, 1989; Pollak *et al.*, 2002, 2003; Shneiderman and Oliver, 1989; Shneiderman *et al.*, 1988) and subsequently from the ICC to the MGB (Peruzzi *et al.*, 1997; Winer *et al.*, 1996). The local inhibitory circuitry in various brainstem/midbrain centers also plays a critical role for refining receptive field preferences by sharpening spectral tuning, sound level sensitivities, binaural preferences, or refining neuronal selectivity to specific temporal sound components (Batra and Fitzpatrick, 2002; Casseday *et al.*, 1994; Davis and Young, 2000; Kuwada *et al.*, 1997; Le Beau *et al.*, 1996). Additional inhibitory processes are evident in AI. Cortical inhibition is responsible for adjusting spectral tuning and enhancing temporal preferences (Wehr and Zador, 2003), including directional preferences for FM sweeps (Zhang *et al.*, 2003).

Due to the vast amount of central inhibition in the ascending lemniscal pathway, numerous techniques have been developed to characterize how inhibitory processes contribute to neuronal sensitivities. These include simple two-tone receptive field measurement techniques, the use of bandpass and broadband noise to activate spectral inhibition, and more intricate methods with complex sounds that attempt to quantify spectral and/or temporal aspects of inhibition. While these indirect receptive field mapping techniques generally do not identify the direct source of inhibitory input, they are nonetheless useful for characterizing how spectral preferences are sculpted across multiple levels of processing.

A. SRAs Probed with Narrowband Stimuli

A variety of approaches have been used to quantify neuronal sensitivities to spectral peaks and notches. Measures of two-tone interactions are perhaps the simplest way to measure the combined influence of spectral excitation and inhibition (Brosch and Schreiner, 1997; Calford and Semple, 1995; Egorova

et al., 2001; Portfors and Wenstrup, 2002; Shamma *et al.*, 1993). A two-tone frequency response curve can be constructed by presenting a reference tone-pip simultaneously with a probe tone-pip of variable frequency and level. The reference tone-pip is often presented at the neuron's CF and an SPL that evokes a strong excitatory response. The complex interactions between the probe and reference tones may in fact have a number of possible outcomes. Generally speaking, the probe tone may have either an excitatory or inhibitory effect on the response to the reference tone. Excitatory interactions may be either *additive*, i.e., the response to the reference and probe is simply the sum of the responses for both of these components, or *facilitative*, in which case the response to the reference and probe tone is greater in magnitude than the sum of responses resulting from each individual component (Egorova *et al.*, 2001; Portfors and Wenstrup, 2002).

Functional inhibition is encountered whenever the firing rate to the reference and probe tone-pips is less than the firing rate for the reference tone alone. The arrangements of inhibition in two-tone frequency response maps have been used as a marker for categorizing SRF properties according to a number of stereotyped inhibitory interactions (Egorova *et al.*, 2001). Two-tone response profiles can exhibit (1) primary-like response areas with narrow excitatory tuning near threshold and broad low frequency tuning at high sound levels or (2) narrowband excitatory tuning with strong flanking sideband inhibition. Classifications of spectral preference have also been based upon inhibition of spontaneous activity profiles. Inhibition of spontaneous activity in decerebrate cats (Ramachandran *et al.*, 1999) can be used as a marker for spectral integration properties in the ICC that resemble those of the brainstem inputs from the DCN, anterior-ventral cochlear nucleus (AVCN), and superior olivery nuclei (SO). Because of functional similarities in spectral sensitivity between colliculus and brainstem inputs (Davis *et al.*, 1999), Ramachandran and colleagues (Ramachandran and May, 2002; Ramachandran *et al.*, 1999) have argued for an inheritance principle in generating ICC receptive fields (see chapter by Davis). Similar functional relationships may also hold for the construction of thalamic and cortical receptive fields from their brainstem and midbrain inputs although the details of this projection are not so well understood.

B. SRFs Probed with Broadband Sounds: Tone-Noise Interactions

The influences of spectral excitation and inhibition have also been measured with a variety of broadband stimulus paradigms. Ehret and colleagues (Ehret and Merzenich, 1985, 1988b; Ehret and Schreiner, 1997) employed a tone-noise masking paradigm to measure spectral filter resolution in the cat ICC and AI. Their procedure is conceptually analogous to psychophysical paradigms

used to measure perceptual filter bandwidths, in which a pure tone is masked by a narrowband noise of variable bandwidth and level. In contrast to pure-tone tuning properties, bandwidth measurements using this technique exhibit level-invariant resolution that closely approaches critical-band masking phenomena and are in agreement with psychophysical measures (see Section IV.D).

C. SRFs Probed with Broadband Sounds: Stationary Spectral Ripples

Spectral ripples are broadband noise with a sinusoidal spectrum that resembles the spectra of communication signals. Spectral ripples have been used to assay excitatory and inhibitory RF properties in AI (Calhoun and Schreiner, 1998; Kowalski *et al.*, 1996; Schreiner and Calhoun, 1994; Versnel and Shamma, 1998). Ripple noises contain peaks and notches in their spectrum at different resolutions and provide a means of systematically manipulating the sound spectral content. The spectral resolution of a peak-notch combination is characterized by the ripple density (Kowalski *et al.*, 1996; Schreiner and Calhoun, 1994) or equivalently the spectral modulation frequency (Miller *et al.*, 2002) (expressed as the number of spectral peaks per octave frequency; cycles/octave). Higher ripple densities correspond to higher spectral resolutions whereas a ripple density of 0 corresponds to a flat spectrum noise. Ripple noise SRF measurements typically exhibit an excitatory component about the BF and often exhibit alternating regions of flanking inhibition above and/or below the BF. Such a receptive field description is conceptually appealing as it parallels the sound spectrum that the neuron prefers (Versnel and Shamma, 1998). This sensitivity could also be expressed as a tuning function with respect to the ripple density parameter, in which case the response is characterized by a response peak at the preferred spectral resolution/ripple density. In the cat and ferret, the inhibitory component of spectral tuning can be asymmetrical such that flanking inhibition appears to be most prominent at frequencies below or above the BF (Kowalski *et al.*, 1996; Schreiner and Calhoun, 1994; Versnel *et al.*, 1995), although in general a variety of arrangements are possible. A related technique using *random spectrum stimuli* (RSS) (see Chapter 6) has revealed similar SRF arrangements in the cat DCN (Yu and Young, 2000) and primate AI (Barbour and Wang, 2003). As for the tone-noise masking studies of Ehret and colleagues (Ehret and Merzenich, 1988b; Ehret and Schreiner, 1997) SRF measurements with broadband ripples and RSS noise are much more level-tolerant than with pure-tone (Barbour and Wang, 2003), which suggests different functional principles underlying the encoding of broadband stimuli.

The prevalence of sideband inhibition observed across many stations in the auditory system has lead to a prevailing view that flanking inhibition about the

CF refines spectral tuning. Two models have been postulated for the arrangement of spectral inhibition that could account for such an observation. On the one hand, inhibition could be confined to flanking regions that extend above and below the central CF region. Such a model would suggest that the inhibitory and excitatory SRF (iSRF and eSRF, respectively) do not fully overlap, but instead are confined to different frequencies. Conversely, inhibition could overlap the entire eSRF and could potentially extend beyond the dominant eSRF region. The arrangement of the excitatory and inhibitory synaptic conductances has been recently measured intracellularly in rat AI and the data support the second model (Wehr and Zador, 2003; Zhang *et al.*, 2003) (Fig. 2). The excitatory and inhibitory SRF of AI neurons are primarily overlapped with similar spectral tuning and high-frequency role-offs, although inhibition is generally temporally delayed relative to the excitation.

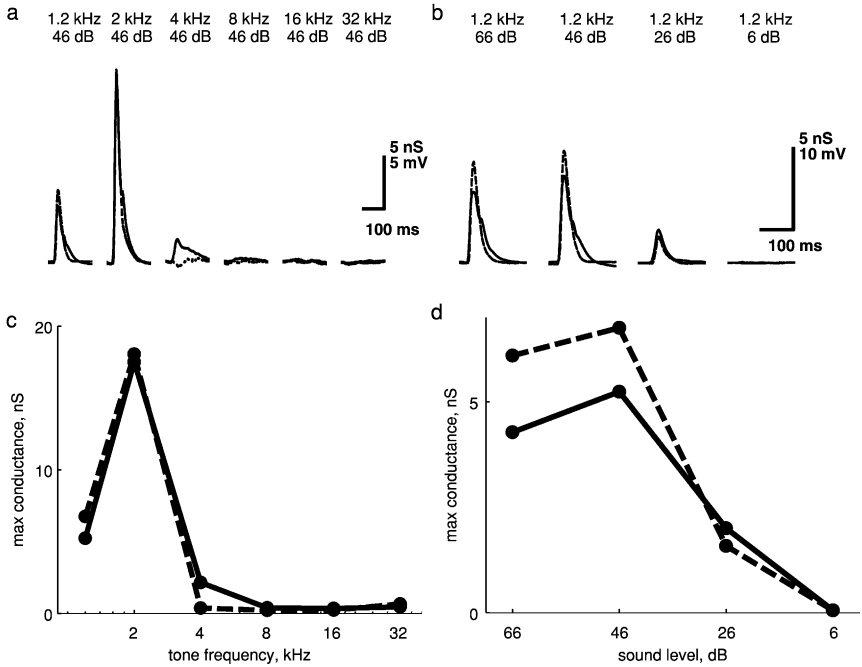

FIG. 2. Excitatory and inhibitory synaptic conductances in the rat auditory cortex are co-tuned for frequency and sound level. (a,b) The excitatory (solid line) and inhibitory (dotted line) synaptic conductances of a neuron with best frequency around 2 kHz show similar timing and amplitude pattern. (c,d) The peak excitatory (solid) and inhibitory (dotted) conductances share similar tuning for frequency (c) and level (d). (Adapted with permission from Wehr and Zador, 2003; Nature Publishing Group).

D. Spectral Resolution and Critical Band Phenomena

Identifying the physiological substrate for perceptual phenomena is a key goal for relating neuronal coding and perception. A number of neuronal mechanisms have been identified in the colliculus, thalamus, and cortex that correlate with critical band spectral integration.

Within the ICC, the frequency gradient of the cochlea is systematically mapped into an array of parallel frequency-band lamina (Merzenich and Reid, 1974; Semple and Aitkin, 1979) (see Section VI.C, Fig. 8. Electrode penetrations along this principal frequency axis of the ICC have demonstrated stepwise 175 μm spacing changes in dominant CF across the lamina. Each lamina encodes for approximately 1/3 octave range of frequencies (Schreiner and Langner, 1997). Such an organization of spectral RF preferences may provide a functional and anatomical substrate for the critical band perceptual resolution. Single neurons in the ICC also exhibit other spectral sensitivities that are consistent with critical band integration. The limiting spectral resolution to pure tones measured in the presence of a noise-masker (Ehret and Merzenich, 1985, 1988b) or to broadband dynamic ripples (Qiu *et al.*, 2003), for instance, mirrors critical band integration.

Critical band resolution phenomena are not exclusive to the ICC. The spectral resolution of the thalamocortical system also approximates critical band integration under a variety of broadband conditions. In cat AI spectral RF measures with both tone-noise masking paradigm (Ehret and Schreiner, 1997) and dynamic ripples (Miller *et al.*, 2002) exhibit spectral sensitivity consistent with 1/3 octave integration. In the awake ferret, Fritz *et al.* (2003) demonstrated that rapid task-related changes in AI receptive fields are confined to approximately 1/3 octave frequency range. This frequency-limited adaptive reorganization of the STRF structure during active learning is consistent with the functional resolution of a subset of thalamocortical projection neurons from the MGBv to AI (Miller *et al.*, 2001; Read *et al.*, 2004). The majority of synaptically connected thalamic and cortical neuron pairs exhibit a high-level spectral alignment within roughly one critical band (Miller *et al.*, 2001). The fact that critical band phenomena along the collicular-cortical pathway invariably require broadband noise conditions might suggest that central inhibition partly underlies these phenomena.

V. Spectral and Temporal Integration

Timing differences in the delay and duration of neuronal excitation and inhibition have a significant impact on the way a neuron responds to a dynamic stimulus. The temporal response pattern of a neuron is not only dependent on the

spectral content of a sound but is also affected by the temporal evolution of the stimulus. Neurons in the DCN and beyond are selective for the spectro-temporal content of the sound.

Inhibition shapes spectral selectivity and also refines temporal aspects of the response at the level of the ICC and above (Casseday *et al.*, 1994, 2000; Kuwada *et al.*, 1997; Wehr and Zador, 2003; Zhang *et al.*, 2003). Temporal response patterns can be measured independently of spectral tuning with repetitive clicks, noises, or sinusoidal amplitude modulated tones (SAMs). Neurons can exhibit tuning to the sound modulations, both on the basis of temporal synchronization (phase-locking) or firing rate. In the ICC, neurons that synchronize to the temporal envelope have been reported to exceed several hundred Hertz, whereas tuning on the basis of firing rate has been demonstrated for modulation rates beyond 300 Hz (Langner and Schreiner, 1988; Rees and Møller, 1987; Schreiner and Langner, 1988). Cortical neurons, on the other hand generally lose synchronization at modulation rates beyond 25 Hz (Eggermont, 1999; Liang *et al.*, 2002; Schreiner and Urbas, 1988). Although such findings confirm a clear transformation of temporal preferences beyond the ICC, a similar transformation for spectral features of a sound has not been clearly identified.

A. FM Sweep Selectivity

Measurements of the dynamics of spectral tuning have been performed under a variety of stimulus conditions. The interdependence between spectral and temporal attributes can be quantified with sounds that vary simultaneously along time and frequency. FM tone sweeps are one such stimulus in which the frequency content is continuously incremented or decreased with time. Measurements of FM selectivity have confirmed that spectral tuning is generally not a stationary response property. In the ICC and above, neurons can exhibit a preferred frequency sweep velocity (number of frequency units traversed per unit time) and direction (low to high versus high to low frequency) (Creutzfeldt *et al.*, 1980; Eggermont, 1994; Heil, 1997b; Kowalski *et al.*, 1995; Mendelson *et al.*, 1993; Nelken and Versnel, 2000; Poon *et al.*, 1990; Rees and Møller, 1983; Versnel *et al.*, 1995; Zhang *et al.*, 2003). Consistent with temporal modulation preferences, neurons in the ICC are sensitive to high frequency sweep velocities and this sensitivity is systematically reduced to lower velocities at AI (Creutzfeldt *et al.*, 1980; Poon *et al.*, 1991; Rees and Møller, 1983). This stimulus specificity to the time-varying spectral content is partly attributed to the temporal interplay between neuronal excitation and inhibition (Casseday *et al.*, 1994; Wehr and Zador, 2003; Zhang *et al.*, 2003). A distributed neural representation for FM sweep or modulation rate may exist at the level of AI (Mendelson *et al.*, 1993; Nelken and

Versnel, 2000; Versnel *et al.*, 1995), however, a similar distribution or topography has not been described for ICC or MGBv.

B. Two-Tone Spectro-Temporal Interactions

Spectro-temporal interactions can also be probed with time-varying tone-pip patterns. In the cat AI, the dynamics of two-tone interactions have been measured during a forward-masking paradigm where the response of a delayed probe-tone of variable frequency and level is masked by a reference tone at the CF and at a fixed level (Calford and Semple, 1995; Brosch and Schreiner, 1997). The exact shape of a two-tone FRA is largely variable upon the delay in which the spike activity is measured. Suppression of excitation usually follows the primary excitatory response at the CF. The average time scale of forward inhibition was approximately 150 msec suggesting a relatively slow time course of forward masking in AI. The spectral extent and timing of cortical neurons found in these studies is in close agreement with perceptual measures of forward masking in humans (Jesteadt *et al.*, 1982).

C. RFs Probed with Broadband Sounds—Dynamic Spectral Ripples

An alternative paradigm for measuring the RF preference is to employ a variety of structured sounds that encompass a wide range of acoustic components. Time-varying spectral peaks and notches in the envelope of a sound form important features that are relevant for communication and which are observed in the envelope of natural sounds. Measurements of a neuron's response to a variety of broadband spectrotemporal sound sequences can be used to obtain a more complete description of the STRF properties.

STRFs in the ICC, MGBv, and AI have been measured with a variety of random broadband noise stimuli. Dynamic ripple sounds represent a synthetic class of sounds with sinusoidal spectra and temporal modulations that has been used to systematically probe STRF sensitivities (Depireux *et al.*, 2001; Escabí and Schreiner, 2002; Klein *et al.*, 2000; Kowalski *et al.*, 1996; Miller *et al.*, 2001, 2002; Qiu *et al.*, 2003). Dynamic ripples are a direct extension of static ripple noise but also incorporate time-varying modulations as illustrated in Fig. 3A. The envelope of a dynamic ripple is characterized by a sinusoidal spectrum and sinusoidal temporal envelope with frequency-sweeping spectral peaks. This general class of broadband sounds is theoretically appealing because it offers a complete set of acoustic modulation parameters (spectral and temporal modulation frequencies) that could be used as a building block for constructing an arbitrary complex sound (e.g., vocalizations and speech) (Klein *et al.*, 2000;

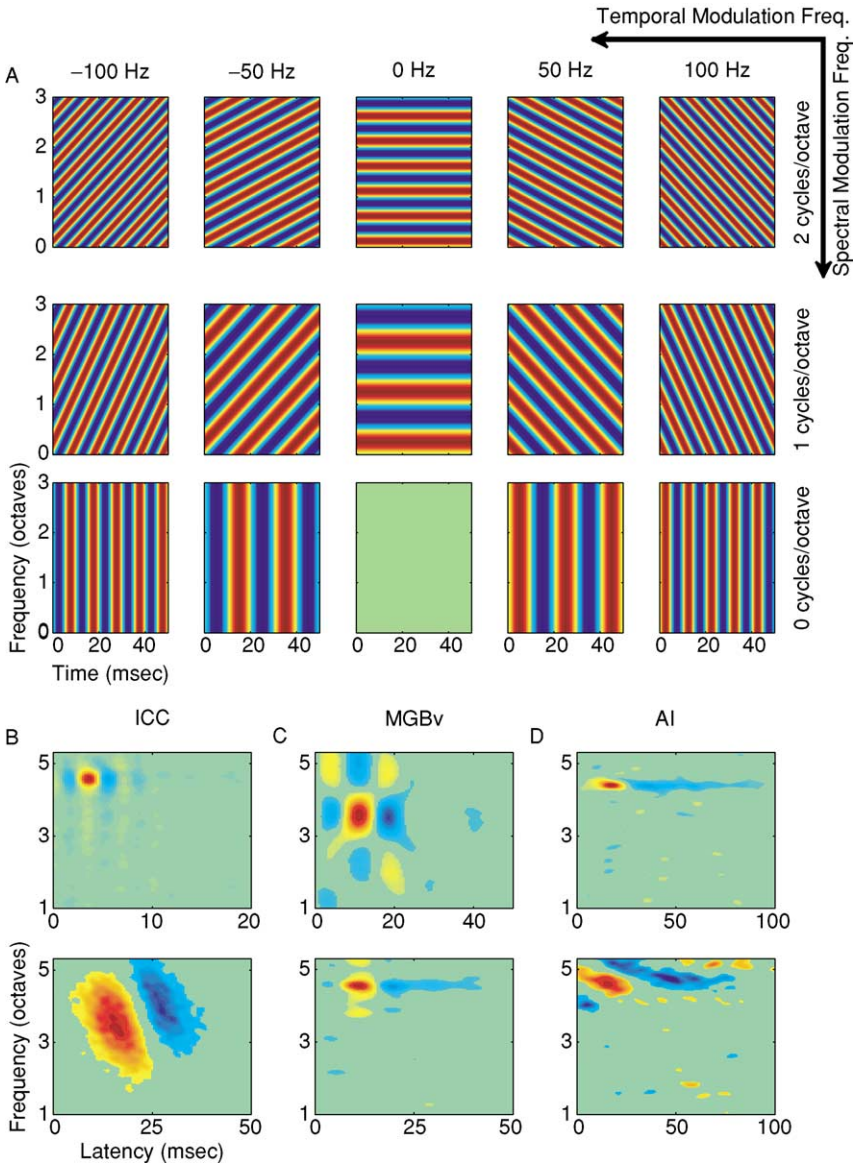

FIG. 3. (A) The spectrotemporal envelope of moving ripple sounds are illustrated as a function of spectral and temporal resolution (SMF and TMF, respectively). Negative SMF produces ripples with upward moving frequency sweeps (top left). Alternately, a high to low frequency transition is observed for ripples with positive SMF (top right). Higher SMF and TMF correspond to finer spectral and temporal resolutions, respectively. Examples of spectrotemporal receptive fields (STRF) from the ICC (B), MGBv (C), and AI (D) were obtained with dynamic ripple sounds. A number of receptive field

Singh and Theunissen, 2003). Although these signals are structurally more complex than simple tone-pips and noise, they are functionally attractive because they offer an intermediate level of complexity that allows for an unbiased assessment of spectral and temporal sensitivities. As illustrated in Fig. 3A the temporal and spectral resolution and ripple sweep direction are controlled by changing the spectral (SMF; units of cycles/octave) and temporal modulation frequencies (TMF; units of Hz). A number of sounds with random spectro-temporal modulations have also been employed for measuring neuronal STRFs. These include random spectrotemporal tone-pips (Blake and Merzenich, 2002; deCharms *et al.*, 1998; Linden *et al.*, 2003; Rutkowski *et al.*, 2002; Theunissen *et al.*, 2000; Valentine and Eggermont, 2004), filtered broadband noise (Escabí and Schreiner, 2002; Keller and Takahashi, 2000; Klein *et al.*, 2000), and natural sounds (Aertsen *et al.*, 1981; Johannesma and Aertsen, 1982; Luczak *et al.*, 2004; Machens *et al.*, 2004; Sen *et al.*, 2001; Theunissen *et al.*, 2000; Yeshurun *et al.*, 1989). In most instances, these are designed so that they retain a flat modulation spectrum and impulsive autocorrelation function within the physiologically relevant range of modulations, thereby satisfying the necessary requirements for estimating STRFs with the reverse correlation technique (de Boer and de Jongh, 1967, 1978; Eggermont *et al.*, 1983; Klein *et al.*, 2000).

The structural arrangement of the STRF can be directly related to the spectrotemporal modulation preferences (Depireux *et al.*, 2001; Escabí and Schreiner, 2002; Klein *et al.*, 2000; Miller *et al.*, 2002; Qiu *et al.*, 2003; Sen *et al.*, 2001) and provides a description of the stimulus features, along time and frequency, which the neuron responds to. Conceptually, the STRF corresponds to the average stimulus pattern that elicited neuronal response. Alternately it could be interpreted as an indirect measure of excitatory and inhibitory RF subregions. Spectrotemporal tuning for neurons in the ICC and beyond is characterized by a variety of arrangements. As for two-tone suppression patterns and for static ripple noise, neurons can exhibit purely excitatory spectral tuning or can exhibit interleaved regions of flanking excitation and inhibition in their STRF (Fig. 3B to D). A variety of temporal arrangements can also be identified. Occasionally, ICC, MGBv, and AI neurons will exhibit a purely excitatory or inhibitory response pattern, but more typically they are characterized by a successive on-off temporal response arrangement. Such temporal patterns could be either independent of the spectral tuning or could exhibit a diagonal time-frequency arrangement suggesting sensitivity to the time-varying frequency content.

---

arrangements are possible: STRF features that are often observed include narrowband versus broadband tuning, presence of sideband inhibition, FM sweep selectivity, temporal inhibition, and/or suppression. In general, a progression from fast to slow timing preferences is observed along the transition from the ICC to AI.

D. STRF Preferences

The relationship between the spectral and temporal components of the STRF can be used to characterize how spectral and temporal aspects of a neuron's integration contribute to a neuron's selectivity. As for direction and motion selectivity in the visual system (Reid *et al.*, 1991), the spectral and temporal components of the integration may interact, leading to selectivity for time-varying components of a sound (e.g., FM sweep velocity and direction). In practice, if temporal RF preferences are independent of spectral preferences, an STRF can be subdivided into a temporal receptive field (TRF) and spectral receptive field (SRF) component from which a neuron's sensitivity could be quantified (Depireux *et al.*, 2001; Qiu *et al.*, 2003; Sen *et al.*, 2001). The SRF or spectral cross-section of the STRF is typically characterized by interleaved patterns of excitation and inhibition and is well approximated by a *Gabor* function (Qiu *et al.*, 2003), i.e., the product of a Gaussian envelope and a sinusoidal carrier. The Gaussian envelope defines the center (BF) and range (bandwidth) over which the neuron integrates spectral information. The sinusoidal carrier accounts for the interleaved spacing of excitation and inhibition and its frequency is closely related to the best ripple density of the neuron (in cycles/octave). A similar decomposition can also be applied to the timing profile of the STRF (Qiu *et al.*, 2003), in which case the Gaussian envelope defines the response duration (Gaussian width) and latency (Gaussian peak) and the sinusoidal component accounts for the best temporal modulation frequency of the neuron (in Hz). In the cat ICC, approximately 80% of the receptive field structure is accounted for with a separable RF model (Qiu *et al.*, 2003), suggesting that spectral and temporal aspects of the integration are largely independent. By comparison, cortical neurons exhibit a greater proportion of inseparable spectrotemporal features (Depireux *et al.*, 2001; Sen *et al.*, 2001) that are consistent with the refinement of directional FM preferences in the cortex (Zhang *et al.*, 2003).

The structural arrangement of spectral and/or temporal excitation and inhibition has also been studied within the context of modulation tuning. The modulation preference of a neuron can be estimated directly from its STRF by Fourier transforming the STRF into a spectro-temporal modulation transfer function (stMTF) (Miller *et al.*, 2002; Qiu *et al.*, 2003; Sen *et al.*, 2001). The stMTF expresses the neurons sensitivity as a function of the sound's temporal (TMF; Hz) and spectral modulation frequency (SMF; cycles/octave or cycles/Hz) (Fig. 4). By considering the arrangement of excitation and inhibition a number of different receptive field preferences can be identified (Miller *et al.*, 2002; Qiu *et al.*, 2003). Temporal *bandpass* tuning occurs whenever the temporal patterning of the STRF has an interleaved arrangement of excitation and inhibition as illustrated in Fig. 4. The temporal MTF exhibits a clear peak at a non-zero best temporal modulation frequency (bTMF). A purely excitatory or inhibitory receptive field

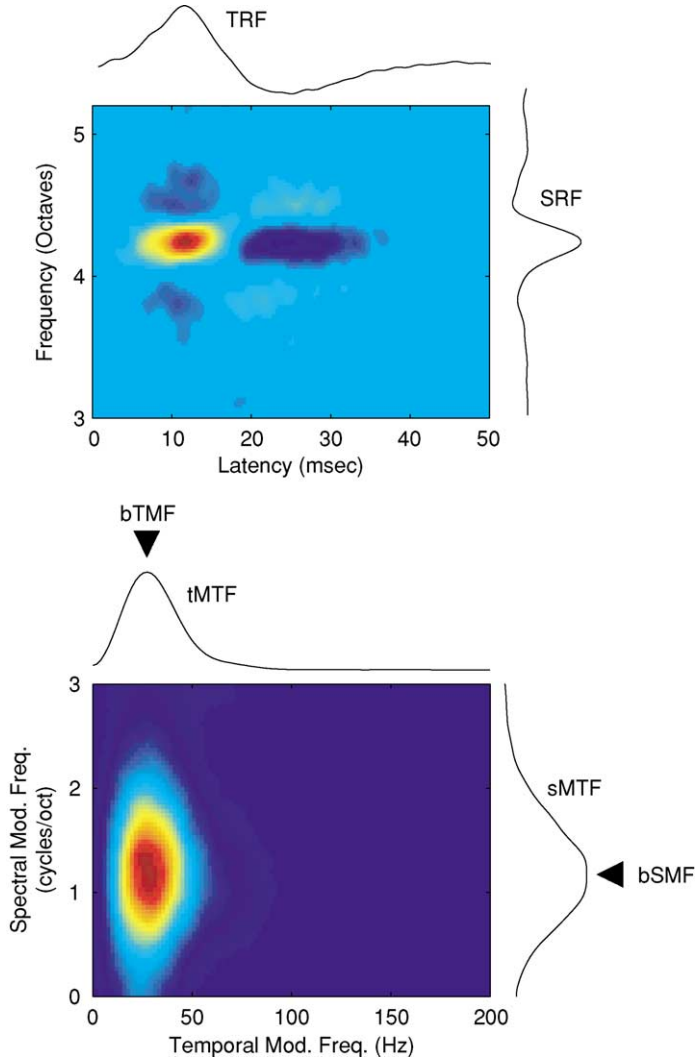

FIG. 4. Spectral and temporal modulation analysis of the STRF preference. A typical ICC receptive field is shown (top) along with its corresponding spectrotemporal modulation transfer function (stMTF) (bottom). The STRF can be decomposed into a temporal receptive field (TRF) and spectral receptive field (SRF) (Qiu *et al.*, 2003). This neuron's TRF is marked by an on-off temporal arrangement whereas its SRF exhibits an off-on-off response pattern. The modulation preference of this neuron can be determined by transforming the STRF to its stMTF, which exhibits a peak response at a preferred spectral and temporal resolution. The spectral and temporal cross sections of the stMTF (to the right and above the stMTF) show a peak about the neurons best temporal modulation (bTMF) and best spectral modulation (bSMF) (denoted by arrows). This neuron responds optimally to 30 Hz temporal modulations and spectral modulations about 1.25 cycles/octave.

temporal pattern, by comparison, will exhibit *lowpass* selectivity. This corresponds to a dominant response at a modulation frequency of 0 Hz. A similar classification scheme can be applied to the spectral sensitivity. Spectral bandpass tuning occurs if the neuron contains flanking sideband inhibition or its stMTF exhibits a best SMF above 0 cycles/octave. Lowpass tuning occurs for a purely excitatory spectral sensitivity, in which case the neuron is sensitive to spectral modulations about 0 cycles/octave (broadband noise).

Consistent with SAM studies, temporal STRF preferences are systematically reduced at each level of the collicular-cortical pathway (Fig. 5A). In the cat, ICC STRFs are characterized by short latency (mean = 10.1 msec; range = 3.5 to 27.4 msec) and short duration (mean = 12.1 msec; range = 1.8 to 82.6 msec) response (Qiu *et al.*, 2003) whereas in the thalamus and cortex the response delays (MGBv mean = 13.2 msec; AI mean = 17.9 msec) are somewhat longer (Miller *et al.*, 2002). Temporal modulation rate measurements from the stMTF reveal that phase-locked modulation rate estimates from STRFs can extend to several hundred hertz in the ICC (Escabí and Schreiner, 2002; Qiu *et al.*, 2003) whereas in thalamus and cortex they are significantly lower (Miller *et al.*, 2002). The mean temporal MTF estimate from the STRF is characterized by bandpass filter profile in all three stations. Furthermore, the best temporal following rate over the population is systematically reduced from 30 Hz at the ICC (observed range = 0 to 255 Hz) to 21.9 Hz and 12.8 Hz in the MGB and AI, respectively (Miller *et al.*, 2002; Qiu *et al.*, 2003). This finding is consistent with temporal modulation studies using SAM and repetitive sequences.

In contrast to temporal preferences, spectral sensitivity in this pathway seems to be much more homogeneous (Fig. 5B). Bandwidth measurements from STRFs reveal a similar range of tuning above the ICC and similar sensitivities to spectral modulations. The average spectral MTF is characterized by a lowpass sensitivity in all three stations (Miller *et al.*, 2002; Qiu *et al.*, 2003) with a peak in the collicular, thalamic, and cortical population MTFs at 0 cycles/octave, suggesting that a large fraction of neurons have little or no sideband inhibition in their STRF, and, therefore, are responsive to broadband stimuli. Furthermore, the range of observed best spectral modulation frequencies (bSMF; observed range = 0 to ~2 cycles/octave) is comparable in all three stations. The limiting spectral resolution estimate from these measurements indicates a maximum resolution of roughly 1/4 octave (1/2 cycle of the maximum observed spectral modulation, ~2 cycles/octave). While the exact nature of these estimates for shaping perceptual resolution still needs further investigation, the limiting STRF resolution in the ICC, MGBv, and AI is surprisingly similar to critical band (1/3 octave) perceptual integration phenomena (Fletcher, 1940; Zwicker *et al.*, 1957).

A unique aspect of the sensory transformation between ICC and thalamocortical receptive field preferences manifests in the combined spectro-temporal population sensitivity. A direct tradeoff in spectral and temporal resolution is seen

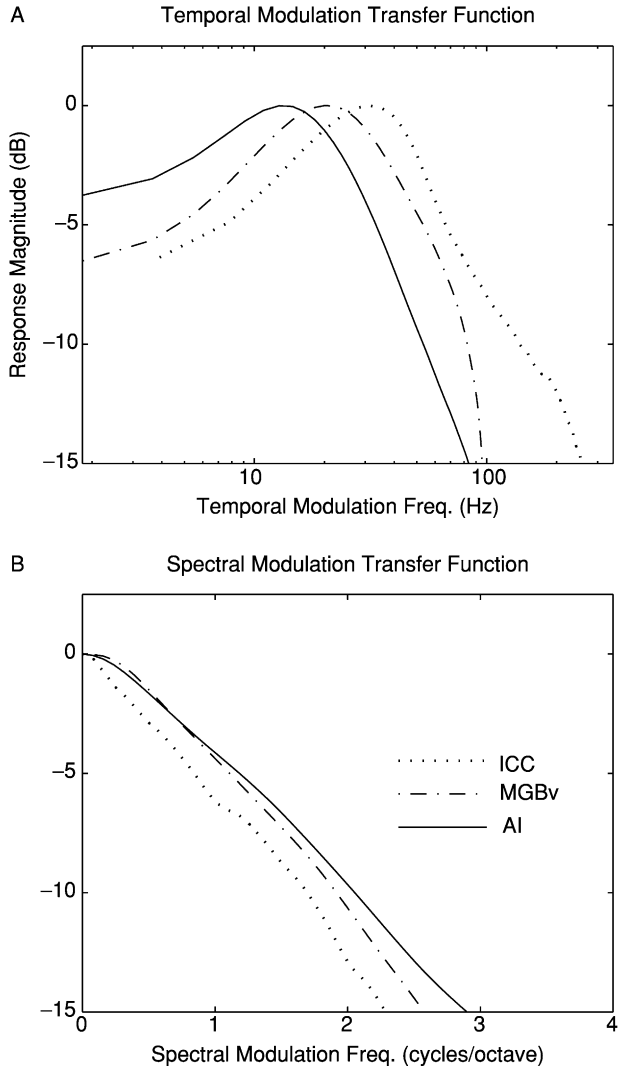

FIG. 5. Population average temporal and spectral modulation transfer functions (tMTF and sMTF, respectively) from the ICC, MGBv, and AI were obtained from the STRF modulation preference (as in Fig. 3). (A) Temporal preferences follow a bandpass selectivity within each station responding optimally to a nonzero temporal modulation. A clear reduction in the preferred/peak temporal modulation rate is observed along the ICC (30 Hz), MGBv (21.9 Hz), and AI (12.8 Hz) pathway. (B) Spectral modulation sensitivity is relatively homogeneous across the three stations, following a low-pass sensitivity with average preferred spectral modulation of 0 cycle/octave (data adapted from Miller *et al.*, 2002 and Qiu *et al.*, 2003).

in the ICC with broadband ripples (Fig. 6) (Qiu *et al.*, 2003) which is not seen using conventional measures of bandwidth or temporal modulation sensitivity. Fast ICC neurons (high bTMF) respond primarily to broad spectral features (low bSMF) while slow integrating neurons are marked by narrow tuning (high bSMF) and strong sideband inhibition. A similar trade-off in spectral and temporal integration resolution has not been observed in thalamic or cortical neurons (Miller *et al.*, 2002). However, there appear to be other forms

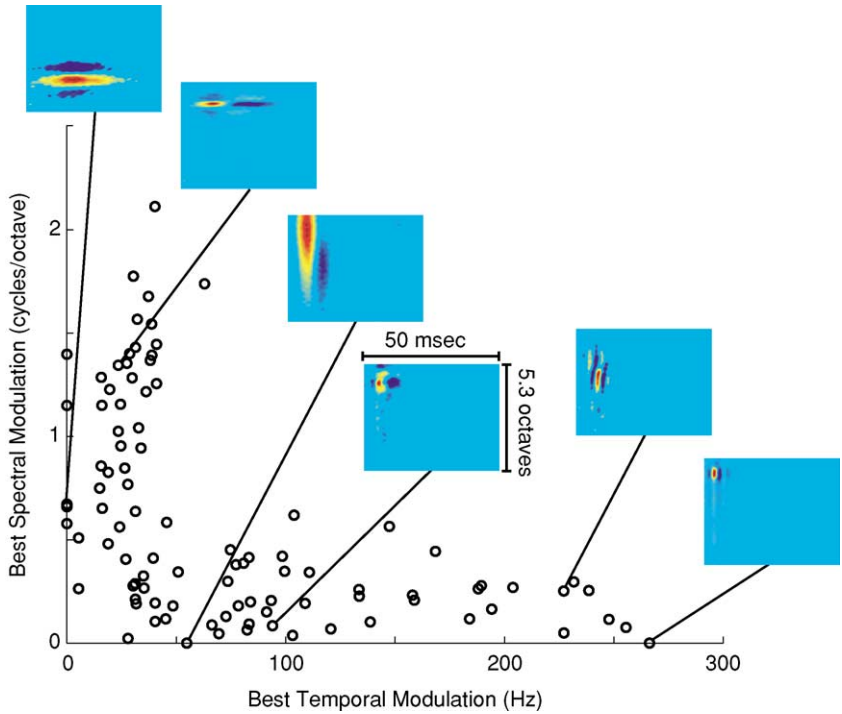

FIG. 6. The best temporal and spectral modulation parameters from ICC neurons exhibit a marked tradeoff in spectral and temporal integration resolution. A similar tradeoff is not observed in the MGBv or AI (Miller *et al.*, 2002; Qiu *et al.*, 2003). Insets show STRFs examples from the ICC at various bSMF and btMF. All STRFs are shown on the same scale (5.3 octave frequency range, ordinate; 50 msec temporal range, abscissa). At fast temporal modulation rates (>50 Hz), ICC neurons are characterized by short temporal duration, fast temporal modulation (Hz), and broad spectral bandwidths. STRFs with high (>50 Hz) modulation rates generally lack spectral sideband inhibition and respond optimally to spectral modulations below 0.5 cycle/octave. Alternately, slow temporal integration neurons (<50 Hz temporal modulation rates) are often characterized by narrow spectral tuning and significant spectral side-band inhibition in the STRF. Neurons with simultaneously high temporal (large bTMF) and spectral resolution (large bSM) are not observed.

of spectro-temporal–dependent properties such as the quadrant non-separability of spectral and temporal components of the STRF for individual neurons (Depireux *et al.*, 2001).

E. Spectral Contrast Sensitivity

Information-bearing components in acoustic signals are often contained within time- or spectral-varying amplitude elements of a complex sound, such as in a peak-notch combination of a vocalization spectrum. The auditory system has an amazing ability to resolve minute differences in amplitude and at the same time is resilient to high levels of background noise and reverberant echoes. It is likely that large peak-to-peak variations observed in natural sounds that are associated with the sound *contrast* may enhance a listener's ability to resolve sounds in noisy environments.

Acoustic contrast can be defined by the peak-to-peak waveform amplitude, waveform standard deviation, or more concisely by the entire amplitude distribution. Thus, contrast is closely related to the sound level and dynamic range. Monotonic and non-monotonic spectral rate-level sensitivities have been described at multiple levels of the auditory system and have been hypothesized as serving as a neuronal correlate for loudness coding. The sound level operating range of a typical auditory neuron (Ehret and Merzenich, 1988a; Evans and Palmer, 1980) is closely matched to the average dynamic range of natural sounds (roughly 30 dB) (Escabí *et al.*, 2003). Thus, it is possible that neurons utilize this operating range not only for level coding but also for encoding spectral and temporal fluctuations associated with the sound contrast. Indeed, AI and ICC neurons can adapt and respond selectively to the dynamic range or contrast of a sound (Barbour and Wang, 2003; Escabí *et al.*, 2003; Kvale and Schreiner, 2004). Neuronal responses to contrast and level are independent suggesting that contrast and loudness coding may in fact involve separate neuronal mechanisms (Escabí *et al.*, 2003).

In most naturally occurring signals, spectral and temporal variations in the instantaneous energy of a sound are normally distributed if defined on a decibel amplitude scale (Attias and Schreiner, 1998b; Escabí *et al.*, 2003). Perceptual studies have demonstrated that loudness perception and discrimination correlate well with the decibel amplitude of a sound but not with its raw sound pressure (Ghitza and Goldstein, 1983; Miller, 1947; Stevens, 1957). Surprisingly, physiological evidence indicates that ICC neurons efficiently utilize decibel fluctuations in natural sounds but are not well suited for encoding linear amplitude differences (Attias and Schreiner, 1998a; Escabí *et al.*, 2003). Furthermore, contrast may serve as a secondary cue for discriminating and categorizing natural signals (e.g., vocalizations and background noise) that have been shown to exhibit

different levels of amplitude contrast (Escabí *et al.*, 2003). While such findings suggest that contrast is an important acoustic parameter, further studies are necessary to identify its exact role in various aspects of neuronal coding and perception (e.g., sound source segregation and discrimination).

VI. Organization of Spectral Receptive Field Properties in Neuronal Populations of ICC, MGBv, and AI

In order to appreciate the transformations in spectral receptive field properties at each successive stage of the auditory sensory pathway, it is important to recognize that there are many processes that serve to alter frequency encoding in the peripheral sensory system. There are at least three anatomically and functionally distinct branches of the lemniscal pathway ascending from the periphery to the auditory brainstem. Indeed, some have suggested more (Thompson and Schofield, 2000). These pathways that have very distinct response properties project to adjacent compartments of the same frequency lamina in the ICC (Oliver, 2000; Oliver *et al.*, 1995). ICC is the primary source for ascending projections to the thalamus that in turn projects to AI. The convergence within and between these pathways very likely underlies many of the spectral transformations that occur between the peripheral sensory ganglia and AI.

A. Cochleotopy from the CN to the ICC

The gradient of cochlear hair cell CFs observed in the cat underlies the cat's extensive frequency audibility range and covers over 10 octaves from 45 to 64,000 Hz (Liberman, 1982; Greenwood, 1990). Cochlear frequency sensitivities are represented topographically throughout the lemniscal auditory pathway. The cochleotopic organization differs among the different branches of the brainstem that project to ICC and thalamus. Furthermore, cochleotopy appears to change with processing level. The primary change in cochleotopy with processing level documented to date is a transition from 1/3 octave laminar separation in ICC to 1 octave laminar separation in MGBv (however, see the caveats described in the following text). Such differences in the cochleotopic organization may be associated with distinct spectral processing tasks along the auditory pathway.

Frequency Organization of Sub-Collicular Input to Central IC: The ICC receives convergent input from three cochleotopically organized sub-collicular nuclei (Fig. 7) (Adams, 1979; Bourk *et al.*, 1981; Irvine, 1992; Saint Marie *et al.*, 1999; Spirou *et al.*, 1993). Dorsal cochlear nucleus (DCN), MSO, and LSO are three major branches of the lemniscal auditory pathway projecting to ICC in

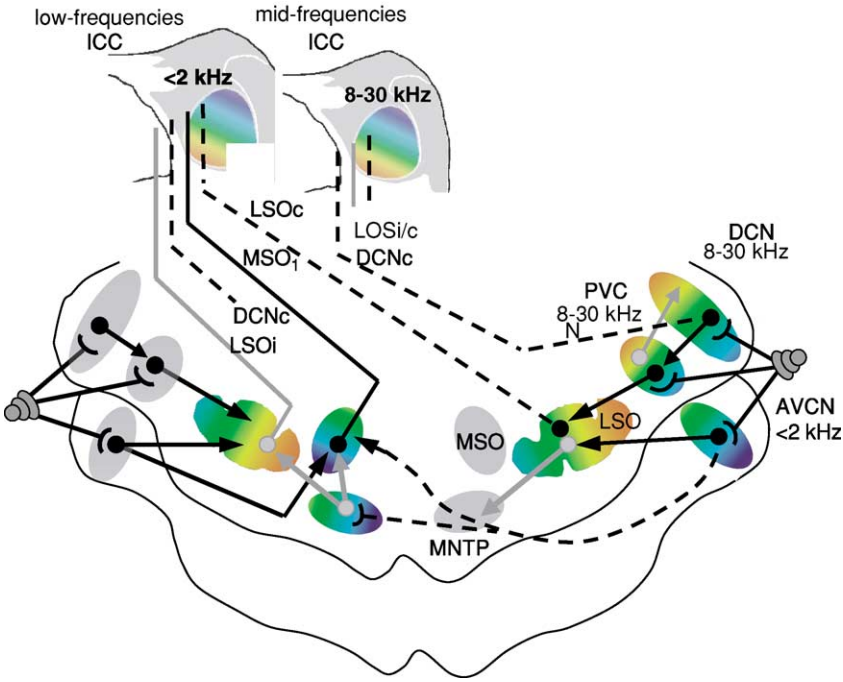

FIG. 7. Major subcollicular pathways projecting to ICC. Each pathway has a separate and in some respects different CF topography. Spiral ganglian input to DCN from two cochlear positions separated by 1 octave is twice the distance for the same octave input in PVCN. Thus, DCN has an expanded area representing mid-frequencies (8 to 30 kHz) whereas PVCN has a compressed area for the same frequencies. DCN inputs go to all iso-frequency laminae in ICC. DCN, MSO, and LSO pathways only project to lower iso-frequency laminae. DCN and LSO pathways project to higher frequency laminae. Direct AVCN/PVCN projections omitted for clarity. DNLL inhibitory projections are not detailed but they cover the same frequency range as LSO. Note that ipsi-hemispheric LSO projections to ICC are inhibitory. This figure is intended to summarize the cochleotopies feeding into ICC and many details have been omitted. Black solid and dotted lines represent excitatory input to ICC. The color scale (blue, green, red, orange) is used to represent the low to high frequency cochleotopic continuum.

mammals.[1] Cochlear sensory ganglion neurons project directly to the ipsi-lateral cochlear nucleus. The CN is functionally and anatomically subdivided into DCN, anterior-ventral (AVCN), and posterior-ventral (PVCN) compartments. The DCN, AVCN, and PVCN have distinct cell populations that are associated with different cochleotopic representations (Bourk *et al.*, 1981; Saint Marie *et al.*, 1999; Spirou *et al.*, 1993).

[1]DCN, MSO, and LSO project to the DNLL which also projects contra-and ipsilateral to ICC.

DCN Pathway: DCN projects heavily to contralateral ICC (dotted line in Fig. 7). The DCN area representing frequencies between 8 and 30 kHz is magnified in size relative to that area representing frequencies below 8 kHz or above 30 kHz (Spirou *et al.*, 1993). A 1/6 octave separation between frequency lamina in DCN corresponds to ~150 μm (Snyder *et al.*, 1997; Spirou *et al.*, 1993). Thus, several frequency laminae in the DCN likely project to a single (1/3 octave) mid-frequency laminae of ICC (Malmierca *et al.*, 1995; Oliver and Morest, 1984; Schreiner and Langner, 1997; Serviere *et al.*, 1984). There are sections of the ICC laminae almost exclusively occupied by DCN terminal fields (Fig. 7) (Oliver, 2000). Furthermore, DCN-like monaural response properties are observed in the ICC and are likely inherited from the ascending synaptic input (Poirier *et al.*, 2003; Ramachandran *et al.*, 1999). In the low iso-frequency laminae of the ICC, DCN input is segregated into a distinct sub-lamina adjacent to MSO/LSO (and DNLL) terminals (Oliver, 2000). Thus, DCN input distributes to appropriate frequency domains but remains relatively segregated within the sub-laminae of ICC.

Functional Distinctions of the DCN Pathway: The DCN pathway clearly plays a role in the spectral integration necessary for processing monaural pinna-based spectral distortions that indicate sound source location relative to the ear and head position (Imig *et al.*, 2000; Oertel and Young, 2004). Spectral properties of local and output projection neurons of the DCN are suited to enhance spectral responses within the middle frequency (8 to 18 kHz) range where pinna distortions in sound spectra are most prominent (Davis and Young, 2000; Imig *et al.*, 2000; Spirou *et al.*, 1999; Young *et al.*, 1992). Response rate for DCN neurons is tuned to spatial location in azimuth and elevation for broad bandwidth sounds; however, the tuning is not observed if probed with narrow bandwidth sounds. Thus, azimuth and elevation tuning in DCN is spectral dependent. A linear relationship between azimuth position, spectral notch, and BF exists for mid-frequency (8 to 18 kHz) projection neurons in the DCN (Imig *et al.*, 2000). Thus, for mid-frequency DCN neurons the cochlear BF reflects spatial location of sound sources! DCN also receives somatosensory input fibers that could carry a neural representation of pinna and head position (Kanold and Young, 2001). Lesions preventing DCN output to higher levels lead to permanent deficits in broad bandwidth spectral-based sound localization tasks (May, 2000).

MSO and LSO Pathways: AVCN and PVCN project directly to the ICC and indirectly to the ICC via the MSO and LSO, respectively (only the MSO/LSO projections are illustrated in Fig. 7) (Adams, 1979). AVCN cochleotopy is complementary to that of the DCN with a greater relative area representing frequencies below 4 kHz (Bourk *et al.*, 1981; Ryugo and May, 1993; Spirou *et al.*, 1993). Cochleotopy in PVCN is approximately one-half the resolution of that in either

DCN or AVCN (Snyder *et al.*, 1997). MSO and LSO have complementary and partially overlapping frequency response property organization (as shown in Fig. 7) (Henkel and Spangler, 1983; Oliver *et al.*, 1995). MSO projects heavily to the low iso-frequency laminae (≤2 kHz) located in dorsal ICC (Fig. 7) (Oliver, 2000; Oliver *et al.*, 1995). MSO and LSO have overlapping terminal field distributions within the low iso-frequency laminae in ICC (≤2 kHz). LSO terminal fields are concentrated in the rostral half whereas MSO terminal fields are concentrated in the caudal half of the laminae (Oliver *et al.*, 1995, 2003). The greatest overlap in MSO/LSO input occurs midway between rostral-caudal borders of the low frequency laminae (labeled "MSO/LSO" in our diagram). LSO projects heavily to the middle and high iso-frequency laminae (=2 kHZ) in ventral ICC. LSO and DCN terminal overlap is greatest for the middle iso-frequency lamina (8 to 18 kHz). However, a sub-laminar segregation is observed for LSO and DCN terminal fields.

Functional Distinctions of the MSO & LSO Pathways: MSO and LSO divisions of the olivary nuclei have some common input from the same cochlear nuclei so a complete functional separation of these pathways is somewhat ambiguous (Fig. 8; Oliver, 2000). However, these sources of converging input have very different functional outcomes as binaural properties in MSO and LSO are quite distinct. MSO neurons process low-frequency sounds and show a distributed code for interaural time (and phase) differences (ITD); whereas LSO neurons process high-frequency sounds and show a distributed representation of interaural level differences (ILD). This fits well with the "duplex theory" of sound localization where low-frequency sounds are localized by timing cues (MSO pathway) and broad bandwidth and high-frequency sounds are located by spectral based ILD cues (LSO pathway) (Middlebrooks and Green, 1991; Populin and Yin, 1998; Pollak *et al.*, 2003; Tollin, 2003). Binaural level differences and spectral shaping of the head-related transfer function are the primary cues for discriminating sound source elevation (Middlebrooks and Green, 1991; Oertel and Young, 2004; Tollin and Yin, 2003; Xu *et al.*, 1999). The latter are likely processed along the DCN and LSO pathways. Thus, MSO and LSO pathways both play prominent roles in processing azimuth while LSO, DCN, and DNLL are important for processing elevation cues. DNLL projections are not shown in Fig. 7. DNLL receives projections from LSO and passes LSO-like response properties to the ICC via long-range inhibitory projections (Pollak *et al.*, 2003). Hence, functionally DNLL can be viewed as part of the LSO pathway. Since the listener and the sound source are often moving in two dimensions (or three) azimuth and elevation cues and the corresponding MSO/LSO pathways likely converge at some level of the auditory pathway in order to generate a cohesive percept.

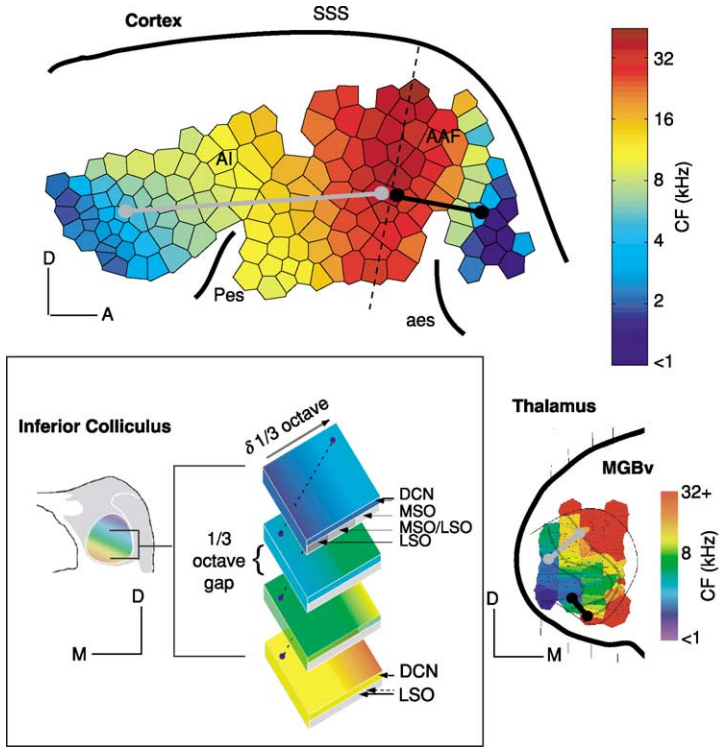

FIG. 8. Multiple cochleotopies in the lemniscal auditory pathway. Rainbow color spectrum indicates CF for each recording site. Blue and red indicate CFs $\leq$ 1 kHz and $\geq$32 kHz, respectively. Inset: Three-dimensional organization of CF in the IC. CF change is small for tangential shifts along the "iso-frequency laminae" (dorso-medial to ventro-lateral). CF changes step-wise with 1/3 octave shifts along the dorso-ventral dimension. MSO/LSO and DCN all project to different sub-laminae of the same low CF iso-frequency laminae. Only DCN and LSO project to the high frequency CF (e.g., >16 kHz) laminae. Thalamus: Rainbow color spectrum indicates CF. Recording positions of four recording tracks within MGBv of the cat reconstructed from data of Imig and Morel (1985). Notice that the mm distance for one octave of CF in the inferior part of MGBv is smaller than that of the superior MGBv. Anatomical studies also show two cochleotopies in cat MGBv (Read *et al.*, 2004). Cortex: topographic map of CF showing low-to-high CF gradient for AI and a mirror reversed CF gradient for AAF (Imaizumi *et al.*, 2004). Note that the mm distance for one octave in AI is about twice that of AAF. Apparently the coarse cochleotopy in AAF is inherited from inferior MGBv.

B. Parallel Processing in the ICC

Several groups have suggested that the DCN, MSO, and LSO branches of the auditory pathway provide functionally distinct parallel pathways that project to physiologically distinct cell types and anatomically distinct sub-laminae in the

ICC (Batra *et al.*, 1993; Davis *et al.*, 2002; Ramachandran and May, 2002; Ramachandran *et al.*, 1999). Neurons within the ICC cluster according to monaural and binaural response properties (Semple and Aitkin, 1979). Monaural and binaural properties could segregate in sub-laminae where DCN and olivary projections to the ICC are non-overlapping; however, direct correlations have not been made between physiologic and anatomic sub-laminae (Oliver, 2000). Non-monotonic "O" type ICC neurons are not sensitive to binaural beats and are considered monaural cell types likely inherited from the DCN pathway (Ramachandran and May, 2002). Type "O" cells would include neurons with monaural azimuth position tuning (Poirier *et al.*, 2003). Azimuth tuning in the ICC is shaped by spectral inhibition which is strongest at the cells own pure-tone BF for mid-frequency neurons as is the case for DCN neurons (Davis *et al.*, 2002; Nelken and Young, 1994; Poirier *et al.*, 2003). Spectral and binaural properties including CF of type "V" and type "I" neurons in the ICC are likely inherited from MSO and LSO projections, respectively (Ramachandran and May, 2002; Ramachandran *et al.*, 1999). Type "I" ICC neurons have binaural sensitivities and are sensitive to binaural beats (Ramachandran and May, 2002). Many neurons with type "I" sensitivity are also sensitive to envelope modulations (Batra *et al.*, 1993). Type "I" class would also include binaural azimuth tuned neurons that have ILD sensitivity but lack the spectral inhibitory properties observed for the DCN pathway neurons (Delgutte *et al.*, 1999; Poirier *et al.*, 2003). The ILD sensitivity of binaural azimuth tuned neurons resembles that of LSO neurons (Poirier *et al.*, 2003). A fourth type of neuron is found in the low iso-frequency laminae and has physiologic properties like both MSO and LSO neurons (Batra *et al.*, 1993; Davis *et al.*, 1999; Ramachandran and May, 2002). The ICC neurons with "dual MSO/LSO properties" may be generated in the ICC via convergence of the two input pathways onto single low-frequency laminae or alternatively via intra-laminar ICC stellate neurons (Biebel and Langner, 2002; Oliver and Morest, 1984). However, a subset of the low- and high-frequency dual spectral sensitivities including envelope modulation sensitivities in the ICC are related to monaural cues possibly due to distortions of frequency sensitivities on the cochlea itself (McAlpine, 2004). Thus, in the future we may speak of a "second order" cochleotopic organization that accounts for a subtype of envelope modulation sensitivities in low-frequency neurons that are related to high-frequency cochlear distortions.

Spectral differences in these different acoustic pathways are intimately related to sound location cues including the processing of binaural versus monaural cues. The degree to which these functional streams remain segregated at various levels remains unclear. Many subcollicular properties are conserved in sub-compartments of the ICC (Davis *et al.*, 1999; Ramachandran and May, 2002; Ramachandran *et al.*, 1999). However, it is clear that some physiologic and anatomical convergence occur between the sub-collicular pathways at the level

of ICC. Intrinsic inhibitory processes within the ICC can refine binaural and monaural response properties including sharpening rate-level dependence, ITD, and ILD sensitivity (Kuwada *et al.*, 1997; Park and Pollak, 1993; Pollak and Park, 1993). For example, cross-hemispheric inhibitory input from DNLL to ICC neurons converges with LSO excitatory input in ICC to create excitatory-inhibitory responses to binaural sound presentation (Burger and Pollak, 2001). This circuitry conserves and recreates similar binaural excitatory-inhibitory properties observed in LSO and creates de novo an inhibition that appears to allow for temporal adaptation to echoes and accurate sound localization (Pollak *et al.*, 2003). A shift from predominantly monaural azimuth tuning to binaural azimuth tuning at the level of thalamus indicates a large degree of convergence between ICC and thalamic levels of the system (Clarey *et al.*, 1995; Poirier *et al.*, 2003; Samson *et al.*, 2000).

Sub-classes of receptive fields have also been identified in the ICC on the basis of linear and non-linear spectrotemporal integration (Escabí and Schreiner, 2002; Escabí *et al.*, 2003), receptive field resolution, and binaural interactions (Qiu *et al.*, 2003). Approximately 1/3 of colliculus high-frequency neurons exhibit significant binaural STRFs (i.e., for the contralateral and ipsilateral sound). The arrangement of excitatory and inhibitory spectrotemporal interactions in the ICC is well suited for processing binaural disparities in the mid- to high-frequency range (Qiu *et al.*, 2003). Monaural neurons likely arise via projections from the DCN whereas binaural interactions in the mid- to high-frequency stream likely arise via the LSO. The spectrotemporal tuning of ICC receptive fields extends from very narrow bandwidth tuning ($\sim$1/3) and slow temporal integration to fast temporal integration and broad bandwidths (Fig. 6). These differences in temporal and spectral resolution could be related to different types of converging inputs from brainstem nuclei (Ramachandran *et al.*, 1999). Alternately, it is plausible that morphological differences in cell class, e.g., stellate versus disk-shaped cells (Oliver and Morest, 1984), or differences in synaptic integration properties (Peruzzi *et al.*, 2000) could contribute to various receptive field classifications. There are presently no studies relating these STRF classifications to the anatomical compartmentalization in ICC or to other conventional receptive field approaches.

C. Three-Dimensional Cochleotopy in ICC

Cochleotopy in the ICC has two axes for frequency organization in three dimensions. Several techniques have confirmed a coarse low-to-high frequency (and CF) organization with dorso-lateral to ventro-medial progression in the ICC (Malmierca *et al.*, 1995; Merzenich and Reid, 1974; Semple and Aitkin,

1979) (Fig. 8). Close examination of recorded CFs along dorso-ventral oriented electrode tracks reveals a ~175 μm frequency laminae where CFs change minimally. A 1/3 octave gap in frequency representation is observed physiologically between adjacent laminae (Schreiner and Langner, 1997) and is consistent with the anatomically defined dorso-medial ventral-lateral laminar organization (Malmierca *et al.*, 1995; Oliver and Morest, 1984). When recording positions are shifted tangentially and recordings are performed along the extent of the frequency laminae (dorso-medial to ventro-lateral) a shallow gradient in CF is observed accounting for the 1/3 octave gap in the dorso-ventral dimension (see δCF axis in Fig. 8). Thus, there is one axis for small changes in CF and another for large changes. These two axes for small versus large changes in CF form a "zig-zag" pattern as illustrated in Fig. 8. A consequence of this pattern is that two very different patterns of CF convergence occur within a radius of ~200 μm. First, disc-shaped neurons with their dendrites restricted to the same iso-frequency laminae interact with neighboring neurons that have very similar CFs. Disc neurons project in parallel to the MGBv and likely conserve the fine resolution cochleotopy of the δCF axis (Fig. 8). Second stellate neurons with dendrites spanning multiple iso-frequency laminae (Oliver and Morest, 1984) are positioned to integrate CFs shifted by =1/3 octave (Biebel and Langner, 2002; Schreiner and Langner, 1997). The dual axes of CF cochleotopy could reflect the formation of new as well as inherited forms of spectral integration in the ICC.

Topographic Spectral Bandwidth Organization of ICC: Spectral bandwidth probed with pure-tones varies topographically across the middle frequency iso-frequency laminae of IC. Bandwidth and CF are spectral properties that can vary independently. When dynamic noise stimuli or pure-tones are used to probe excitatory bandwidths of the STRF, the majority of neurons in ICC respond to a narrow range of frequencies spanning approximately ±1/4 of an octave while a smaller proportion of broadly tuned transient neurons respond over several octaves beyond their CF or BF (Qiu *et al.*, 2003) (see Fig. 6). Such response profiles are consistent with the anatomic restriction of disc cell dendrites to ~175 μm (Oliver and Morest, 1984) and the hypothesis that broad spectral selectivity can be created across laminar integration of stellate neurons. Thus, two neurons displaced in the anterior-posterior dimension of the same iso-frequency laminae can share the same CF but have very different pure-tone bandwidths. Two mirror-symmetric (concentric) gradients for bandwidth extend from the center of an iso-frequency laminae to the respective borders (Ehret *et al.*, 2003; Schreiner and Langner, 1988). Narrow-to-broad bandwidth gradients in the ICC could be generated by a gradient of DCN versus LSO terminal fields to the mid-frequency laminae; however, no such direct correlation has been demonstrated.

D. Cochleotopic Transformations or Heterogeneity in the MGBv

Recently it has been suggested that dramatic changes in cochleotopy occur between the level of ICC and the MGBv division of auditory thalamus (Cetas *et al.*, 2001, 2003). A dramatic difference in cochleotopy could allow for similarly dramatic differences in spectral processing. Unfortunately, this hypothesis is largely derived from comparisons made across species. Namely, McMullen *et al.* recently presented both anatomic and physiologic evidence that discrete 1-octave jumps occur between adjacent iso-frequency laminae in rabbit MGBv. Since the primary input to MGBv is from the ICC, the data may indicate a major transformation in spectral representation between the two stages. Alternatively, the 1-octave cochleotopy in MGBv could be inherited from brainstem projections of the ICC or DCN. Unfortunately, there is little published data supporting a 1-octave MGBv cochleotopy in mammals other than the rabbit. Early physiologic studies of frequency lamina organization in the cat MGBv demonstrated a low-to-high CF gradient with a lateral to medial progression in MGBv (Fig. 8). The cat MGBv iso-frequency laminar organization for one case of Imig and Morel's original physiologic data (Imig and Morel, 1985) is reconstructed using vornoi tessellation and color coding to indicate CF for each recording site. This reconstruction hints at different cochleotopies in central MGBv and inferior parts of MGBv. In central MGBv, many adjacent frequency contours can be physiologically resolved. This high-resolution cochleotopy could be essentially inherited unchanged from the 1/3[2] octave iso-frequency laminae of ICC. In contrast, the inferior aspect of MGBv appears to have a coarse laminar separation resembling that seen in the rabbit MGBv. Unfortunately, it is hard to quantify the cochleotopy differences in the Imig and Morel data because the reconstruction includes only four electrode tracks separated by more than 700 μm.[3] Recently, several anatomic and physiologic distinctions between central and inferior domains of MGBv have been described (Read *et al.*, 2004). First, a difference in cellular morphology and cochleotopy is observed for central versus inferior MGBv. Inferior MGBv has a coarse cochleotopy similar to that described for the rabbit MGBv. Distinct physiologic properties have been attributed to central and inferior MGBv (He, 2002; He and Hu, 2002). The central versus inferior compartments of MGBv defined by cochleotopic differences may correspond to these previously described sub-compartments.

Physiologic Distinctions of MGBv Subdomains within the Iso-Frequency Dimension: The degree of ICC convergence between DCN-, MSO-, and LSO-dominated subcompartments as they project to MGBv is unknown. Binaural and monaural

[2]1/3 octave lamina have only confirmed for 4 to 20 kHz. (Schreiner and Langher, 1997).

[3]A fine scale reconstruction of the laminar profiles in cat MGBv is more difficult than the rabbit due to the 90 degree rotation in the frequency lamina axis.

response properties are known to segregate along the superior-to-inferior dimension of MGBv. Unfortunately, the methods of characterizing binaural/monaural properties in DCN and ICC are generally different than those used for MGBv neurons. For this reason, it is difficult to describe topographic or organizational differences in cochleotopy in the MGBv with confidence.

Sharpening and Binaural Integration of Azimuth Tuning to Broadband Sounds in MGB: Central MGBv and rostral pole neurons have sharp binaural azimuth tuning sensitivities which are typically not seen at sub-thalamic levels (Barone *et al.*, 1996; Samson *et al.*, 2000). The spectral-dependent properties of MGBv azimuth tuned neurons likely reflects properties inherited from the "DCN dominated" pathway (Imig *et al.*, 2000; Nelken and Young, 1994). Azimuth tuning of MGBv neurons also changes with binaural versus monaural noise presentation (Samson *et al.*, 1993). Binaural frequency disparity tuning is not seen at the level of DCN and likely reflects the convergence of monaural azimuth representations in ICC.

Sharpening and Binaural Integration of ITD Azimuth Tuning in MGB: MGB neurons have sharper ITD azimuth tuning sensitivities than observed for SO and ICC neurons (Fitzpatrick *et al.*, 1997). Sharpening of ITD tuning in MGB could allow for a more efficient neural population coding of this sound parameter. MGB neurons detect ITDs created by either pure-tones or modulated noise. Thus, the spectral dependence of this form of azimuth tuning in MGBv is more like that of the MSO and LSO pathways than the DCN pathway. Unfortunately, there is little information on whether ITD and ILD cues are independently represented at the level of MGBv.

VII. Primary Auditory Cortical Acoustic Feature Representation and Processing

Auditory cortex can be sub-divided according to cochleotopic organization, spectral integration, azimuth tuning properties, and behavioral effects following lesions. Up to four distinct cochleotopically organized regions have been described in mammalian auditory cortex (Schreiner *et al.*, 2000). Examples of differences in cochleotopic representations are described in the following text and illustrated in part in Fig. 8. A direct correlation between the cochleotopy and specializations in spectral or azimuth tuning for a given population of neurons has not been made; however, clear distinctions in these properties characterize the different auditory cortical regions including primary (AI), anterior auditory field (AAF), and posterior auditory field (PAF). Behavioral studies have demonstrated a critical role for both AI and PAF in making fine scale orientations along the azimuth (Adriani *et al.*, 2003; Jenkins and Merzenich, 1984; Malhotra *et al.*, 2004; Smith *et al.*, 2004). The frequency representation for 5 to 20 kHz is

expanded in AI versus AAF (Imaizumi *et al.*, 2004). AI neurons are azimuth and elevation tuned to broad bandwidth sounds falling in this range and, therefore, at least a sub-popultation of AI neurons is likely to play a role in representing the pinna distortion cues (Barone *et al.*, 1996; Samson *et al.*, 1994; Schnupp *et al.*, 2001; Xu *et al.*, 1998). Azimuth also is represented coarsely in PAF neuron populations (Barone *et al.*, 1996; Orman and Phillips, 1984). The anterior auditory field, on the other hand, does not appear to be critical for locating sound source in space nor have there been any reports of azimuth or elevation tuning in this area. These dramatic differences in functional organization of auditory cortex can be in part attributed to the fact that each cortical region has a unique dominant thalamic source of input. Accordingly, many of the differences in functional organization between auditory cortices could be inherited from their dominant thalamic input. It is a bit more challenging to say exactly what changes in spectral and sound location tuning occur between the level of thalamus and the corresponding cortical target region. In the following, we describe some of these transformations with an emphasis on what emerges in AI and AAF.

A. Cochleotopy and Spectral Integration in AI and AAF

Most physiologic and anatomic studies of cochleotopic organization in AI suggest a homogenous cochleotopy exists at this level of the auditory pathway. A low-to-high CF gradient (cochleotopy) runs from posterior to anterior AI (Fig. 8). AI receives the bulk of its input from the MGBv which is the thalamic subdivision with the highest resolution cochleotopy. The mm of cortex representing the CF gradient for 2 to 32 kHz domain is ~5 mm. For the 4-octave region between 2 and 32 kHz, 1 octave is represented by ~1 mm in the anterior-posterior dimension (Imaizumi *et al.*, 2004; Merzenich *et al.*, 1975). In contrast, the cochleotopy of AAF is very coarse for much of the same range of frequencies (2 to 32 kHz) (Imaizumi *et al.*, 2004). The coarse cochleotopy in AAF is consistent with the fact that this region derives more of its thalamic input from the inferior part of MGBv that appears to have a similar coarse cochleotopy. The inferior MGBv also projects to parts of AI. However, there is no evidence as of yet that the coarse and fine cochleotopies of inferior and central MGBv persist at the level of AI.

B. Bandwidth and FM Organization in AI

A topographic pattern of organization for level-dependent bandwidth and long-range cortical connections is observed in AI. The range of level-dependent responses and corresponding RF bandwidths is extended and represented

topographically in AI as compared to subcollicular stations (Barone *et al.*, 1996; Read *et al.*, 2001). Non-monotonic level dependence is more common and more pronounced in AI than other levels (Barone *et al.*, 1996; Clarey *et al.*, 1995). Neurons with very broad bandwidths covering over five octaves of frequency space are only observed in mature cat AI (Bonham *et al.*, 2004). The developmental dependence of the cortical broadband neurons is distinct from the broad bandwidth tuning seen earlier in development in collicular and sub-collicular neurons. Narrow and broad bandwidth neurons have two extreme operating ranges. Bandwidth is correlated with threshold such that narrow and broad bandwidth neurons have low and high response thresholds respectively (Schreiner *et al.*, 2000). Broad bandwidth neurons have FRAs that increase in frequency range and rate of firing monotonically with sound level whereas narrow bandwidth neurons tend to shut down at the higher sound pressure levels (Phillips *et al.*, 1985; Ramachandran *et al.*, 1999; Schreiner *et al.*, 1992). The extreme differences in operating range may explain why narrow bandwidth domains are not connected to broad bandwidth domains via long-range cortico-cortical connections (Read *et al.*, 2001). In a similar fashion, long-range cortical connections are established between subsets of neurons with similar orientation and ocular dominance tuning in cat primary visual cortex (Gilbert and Wiesel, 1989).

The topographic organization of FM speed tuning and binaural response properties are related to that of the level-dependent bandwidth organization in AI (Heil, 1997b; Kowalski *et al.*, 1995; Mendelson *et al.*, 1993; Versnel *et al.*, 1995; Zhang *et al.*, 2003). Narrow and broad bandwidth neurons correspond in location to those neurons responding to slower versus faster FM modulations, respectively. The functional and anatomic organization related to binaural properties has a different spatial organization than that of bandwidth properties (Middlebrooks *et al.*, 1980). Many of the binaural properties observed in AI are observed within the central narrow bandwidth compartment (Read *et al.*, unpublished). A subset of narrow bandwidth neurons is azimuth tuned for broad bandwidth sounds (Samson *et al.*, 1994). The broad bandwidth neurons in AI may have a more homogeneous monaural or binaural sensitivity since this compartment occupies a relatively smaller area of cortex; however, this has not been demonstrated. There are few if any studies demonstrating topography of ITD, ILD, or broadband spectral-based azimuth tuning of the broad bandwidth neurons. Together these studies would imply that the broad bandwidth neurons are operating at relatively high sound levels and are tuned for faster FM modulations. Conversely, narrow band neurons are operating at relatively low sound levels, are tuned to slow FM modulations, and a subset are likely binaurally tuned to azimuth location. Unfortunately, it is difficult to demonstrate all of these parameters across the $\sim 4 \times 10$ mm area of AI; so no direct comparisons between these feature representations have been made. The value of compartmentalizing and topographically

representing neurons with similar response properties is still unknown. An appealing although disputed explanation for a similar compartmentalization in visual cortices is that it maximizes response feature coverage for any given sensory epithelium position (Carreira-Perpinan and Goodhill, 2002, 2004).

VIII. Physiologic Distinctions or Transformations in AI

A. Level-Dependent Broad Bandwidth Azimuth Tuning

A correspondence between level-dependence and sound source location tuning appears for the first time in AI. Azimuth-tuned neurons in MGBv and AI have non-monotonic level-dependent responses to broadband noise; however, the level dependence is greater for AI (Barone *et al.*, 1996; Clarey *et al.*, 1995). At the levels of DCN and MGBv there is no correlation between level dependence and azimuth tuning (Barone *et al.*, 1996). Azimuth tuning also becomes sharper in AI relative to MGBv (Barone *et al.*, 1996; Samson *et al.*, 2000). Binaural azimuth tuning in AI could arise from: (1) contralateral AI callosal input, or (2) convergence of functional sub-domains of MGBv. The anatomical basis or functional repercussions of this change in azimuth tuning are as yet unknown.

B. Spectral Tuning

Two distinct types of spectral transformations occur in the transition from MGBv to AI. Paired single unit recordings between thalamus and AI cortex reveal two forms of thalamocortical CF convergence. AI properties are deemed "inherited" for thalamocortical neuron pairs with excitatory response area CFs that are matched within 0.05 octaves. AI excitatory CFs are deemed "constructive" for thalamocortical neuron pairs with excitatory response area CFs that are mis-matched by as much as 2/3 octave ($\pm$ 1/3 octave) (Miller *et al.*, 2001). We have hypothesized that inheritance and constructive frequency convergence arise from central and inferior subdivisions of the MGBv, respectively (Read *et al.*, 2004). However, the limited number of correlated (paired) units prevents a thorough population analysis of the anatomical (MGBv sub-compartment) source for the two physiologic convergence patterns.

C. Binaural Properties

The degree to which left and right ear spectral sensitivities are conserved between thalamic and cortical levels of processing is still somewhat of a controversy. Combined anatomical and physiologic studies indicate a high degree of

conservation for many binaural and monaural properties between thalamic neurons and their cortical targets (Cetas *et al.*, 2002; Velenovsky *et al.*, 2003). On the other hand, simultaneous recordings from thalamocortical neuron pairs reveal significant differences in interaural receptive field properties (Miller *et al.*, 2001, 2002). The later studies employed uncorrelated dynamic noise stimuli presented simultaneously to each ear with the same SPL range and variable spectrotemporal content. Differences in the contralateral and ipsilateral STRF structure include CF shifts that may be important for processing binaural spectral disparities in the mid to high frequency range. STRF structure for ipsi versus contra ear inputs can be highly similar, inverted spectrally, or dissimilar in both temporal and spectral character. A similar range of interaural or binaural patterns has been observed for ICC (Qiu *et al.*, 2003). However, interaural pattern for STRFs can be dramatically different for thalamic and cortical neurons that appear synaptically connected based on cross-correlation histogram analysis (Miller *et al.*, 2001, 2002). The latter finding suggests that more than one kind of binaural STRF pattern may converge onto a single layer IV cortical neuron. Thus, at least some cortical neurons do not strictly inherit their binaural pattern. There have been no simultaneous recordings of paired collicular and thalamic neurons to indicate the degree to which binaural properties are transformed between these two levels.

D. Functional Distinctions and Processes Served by AI

Primary auditory cortex (AI) clearly plays a significant role in the spectral integration necessary for sound source location relative to the head (and likely the ear) (Imig *et al.*, 2000; Oertel and Young, 2004). Cats and ferrets with lesions of AI do not orient properly to broad bandwidth noises presented in the contralateral auditory field (Jenkins and Masterton, 1982; Malhotra *et al.*, 2004; Smith *et al.*, 2004). In contrast, lesions of the neighboring anterior auditory cortical fields do not alter orientation to broad bandwidth noises (Malhotra *et al.*, 2004). The orientation deficits seen with AI lesions resemble those observed when DCN projections are interrupted. A subset of neurons in the AI are sharply tuned to sound source location in the azimuth (Barone *et al.*, 1996). A correlation between strongly non-monotonic FRAs and azimuth tuning is observed in the AI but not in the MGBv (Barone *et al.*, 1996; Clarey *et al.*, 1995). Hence, the functional and anatomic compartmentalization of level-dependent narrow bandwidth neurons in AI may be related to pinnae-based spectral integration and azimuth/elevation tuning. However, a correlation between topographic patterns of azimuth/elevation tuning and level-dependent bandwidth has not yet been described in AI. It is also not known if the broad-bandwidth monaural tuned neurons in AI correspond to the neurons with high FM speed selectivity described in the previous text. It is clear that AI has a distributed representation

for spectral and temporal integration (e.g., FM speed selectivity); however, it is not clear if this process is independent of binaural processing.

As previously outlined in detail, there are many spectral properties of AI neurons that can be attributed or related to their binaural properties. FM speed selectivities and level-dependent bandwidth properties in AI traditionally have not been related to binaural RFs. It will be interesting to see if there are parallel and independent mechanisms for representing monaural versus binaural spectral (and temporal) features of sounds within AI.

At some point in the auditory pathway it is likely that extensive convergence of the DCN, LSO, and MSO pathways occurs. The striking and perhaps surprising concept to emerge in both physiologic and anatomic descriptions of the past 15 years is that these pathways remain somewhat segregated even at the level of the ICC. Indeed, clear demonstrations of convergence of these pathways on single neurons within the ICC are rare. These different pathways clearly play different roles in sound source localization and orientation and yet most auditory scenes and sounds will clearly activate these three pathways in parallel. It is likely that these processing streams will converge extensively at some point in the lemniscal pathway to allow for unified auditory percepts of sounds. Hence, it will be of interest to see how and if such convergence occurs in the output of ICC to the level of MGB, AI, or at some point later.

IX. Conclusions

Demonstrating the distinct spectral processing streams in the lemniscal auditory pathway has been a formidable task and yet we still do not fully understand their functional role in sound perception. Perhaps the most fundamental task of the cochlea and the lemniscal auditory pathway as a whole is to decompose sounds into frequency channels that can be further analyzed and processed in central stations. Still, numerous aspects of the functional and organizational principles in central auditory stations remain unresolved. At the early brainstem centers, binaural and functionally distinct monaural pathways remain segregated and cochleotopy is established bottom-up via the cochlear projection. From this point of view, the processes served by individual brainstem nuclei can be described as serving a somewhat well-defined task and function, i.e., spectral and intensity analysis in the CN and binaural processing in the SO. Significant differences in cochleotopy are observed at the earliest stages (e.g., PVCN versus AVCN) and perhaps emerge *de novo* at later stages (e.g., MGBv). These heterogeneities in the distributed representation of spectral RFs are explicable in some cases. For example, SRF and cochleotopic differences in MSO versus LSO can be attributed to the role these neural stations play in extracting given spectral

features. In contrast, no clear function or statistical properties of sound explain the coarse cochleotopy in PVCN, MGBv, or AAF. It has been suggested that PVCN neurons provide a "wide band" inhibition to DCN neurons (Davis and Young, 2000; Nelken and Young, 1994). Perhaps, a similar wide-band cochleotopy and physiologic property is conferred from PVCN to ICC. It has been difficult to demonstrate a novel process sub-served by the ICC (or MGBv for that matter), including the possibility that the ICC extracts monaural or binaural pitch (Langner, 1997; Langner *et al.*, 2002; McAlpine, 2004). At least three functionally and anatomically distinct sub-collicular pathways converge inputs onto adjacent sub-laminae and compartments of the ICC. Clearly, the recipient ICC neurons are in a position to integrate across these functional domains and yet there is little evidence of a clear functional convergence. We can say with confidence that AI plays a role in representing the contralateral spatial location of sounds, but we cannot say if this is due to convergence between MSO/LSO and DCN pathways in MGBv. In general, future studies will be needed to understand the specific functions or processes served by parallel branches versus subsequent levels of the primary auditory pathway.

It remains a challenge to relate the function of the ICC, MGBv, and AI to the ascending, descending, and local anatomical circuitry. Although some functional properties in the ICC appear to be directly inherited from the brainstem inputs (e.g., spectral integration and binaural type) other aspects of the functional organization are constructed *de novo* via the grid of laminar inputs and its subsequent 1/3 octave cochleotopy and bandwidth topography. Emergent cochleotopies and topographies within the ICC, MGBv, and AI have been described on the basis of bandwidth, sound level, temporal properties, and binaurality. As pointed out in Fig. 7, the dual cochleotopies in ICC, MGBv, and auditory cortex may exist in some form in sub-collicular structures. The specific relationships between these topographies and their roles for acoustic processing and perception still need to be determined. There is sufficient evidence to suggest that simple physiologic properties correlate and may be related to specific acoustic processing tasks such as loudness coding and sound localization. Yet, other high-level functions including sound recognition and source segregation have not been directly related to the physiology or anatomy (but see the chapter by Sinex). The use of sophisticated receptive field approaches with more realistic acoustic stimuli, including natural sounds, should help identify functional and topographic distinctions that cannot be seen under the restricted operating regime afforded by pure-tone and white noise conditions. Although physiologic mapping studies alone are revealing new findings about the organization of the central auditory system, it is much more likely that combined anatomical, behavioral, and physiologic studies will yield key insights to the role subserved by distinct spectral processing streams and cochleotopic organization of the lemniscal pathways.

References

Adams, J. C. (1979). Ascending projections to the inferior colliculus. *J. Comp. Neurol.* **183,** 519–538.

Adriani, M., Maeder, P., Meuli, R., Thiran, A. B., Frischknecht, R., Villemure, J. G., Mayer, J., Annoni, J. M., Bogousslavsky, J., Fornari, E., Thiran, J. P., and Clarke, S. (2003). Sound recognition and localization in man: Specialized cortical networks and effects of acute circumscribed lesions. *Exp. Brain. Res.* **153,** 591–604.

Aertsen, A. M., Olders, J. H., and Johannesma, P. I. (1981). Spectro-temporal receptive fields of auditory neurons in the grassfrog. III. Analysis of the stimulus-event relation for natural stimuli. *Biol. Cybern.* **39,** 195–209.

Attias H., and Schreiner, C (1998a). Coding of naturalistic stimuli by auditory midbrain neurons. *Advances in Neural Information Processing Systems* **10,** 103–109.

Attias H., H., and Schreiner, C. (1998b). Low-order temporal statistics of natural sounds. *Advances in Neural Information Processing Systems* **9,** 27–33.

Bajo, V. M., Merchan, M. A., Malmierca, M. S., Nodal, F. R., and Bjaalie, J. G. (1999). Topographic organization of the dorsal nucleus of the lateral lemniscus in the cat. *J. Comp. Neurol.* **407,** 349–366.

Barbour, D. L., and Wang, X. (2003). Contrast tuning in auditory cortex. *Science* **299,** 1073–1075.

Barone, P., Clarey, J. C., Irons, W. A., and Imig, T. J. (1996). Cortical synthesis of azimuth-sensitive single-unit responses with nonmonotonic level tuning: A thalamocortical comparison in the cat. *J. Neurophysiol.* **75,** 1206–1220.

Batra, R., and Fitzpatrick, D. C. (2002). Monaural and binaural processing in the ventral nucleus of the lateral lemniscus: A major source of inhibition to the inferior colliculus. *Hearing Res.* **168,** 90–97.

Batra, R., Kuwada, S., and Stanford, T. R. (1993). High-frequency neurons in the inferior colliculus that are sensitive to interaural delays of amplitude-modulated tones: Evidence for dual binaural influences. *J. Neurophysiol.* **70,** 64–80.

Biebel, U. W., and Langner, G. (2002). Evidence for interactions across frequency channels in the inferior colliculus of awake chinchilla. *Hearing Res.* **169,** 151–168.

Blake, D. T., and Merzenich, M. M. (2002). Changes of AI receptive fields with sound density. *J. Neurophysiol.* **88,** 3409–3420.

Bonham, B. H., Cheung, S. W., Godey, B., and Schreiner, C. E. (2004). Spatial organization of frequency response areas and rate/level functions in the developing AI. *J. Neurophysiol.* **91,** 841–854.

Bourk, T. R., Mielcarz, J. P., and Norris, B. E. (1981). Tonotopic organization of the anteroventral cochlear nucleus of the cat. *Hearing Res.* **4,** 215–241.

Brosch, M., and Schreiner, C. E. (1997). Time course of forward masking tuning curves in cat primary auditory cortex. *J. Neurophysiol.* **77,** 923–943.

Burger, R. M., and Pollak, G. D. (2001). Reversible inactivation of the dorsal nucleus of the lateral lemniscus reveals its role in the processing of multiple sound sources in the inferior colliculus of bats. *J. Neurosci.* **21,** 4830–4843.

Calford, M. B., and Semple, M. N. (1995). Monaural inhibition in cat auditory cortex. *J. Neurophysiol.* **73,** 1876–1891.

Calhoun, B. M., and Schreiner, C. E. (1998). Spectral envelope coding in cat primary auditory cortex: Linear and non-linear effects of stimulus characteristics. *Eur. J. Neurosci.* **10,** 926–940.

Cant, N. B., and Benson, C. G. (2003). Parallel auditory pathways: Projection patterns of the different neuronal populations in the dorsal and ventral cochlear nuclei. *Brain Res. Bull.* **60,** 457–474.

Carreira-Perpinan, M. A., and Goodhill, G. J. (2002). Are visual cortex maps optimized for coverage? *Neural. Comput.* **14,** 1545–1560.

Carreira-Perpinan, M. A., and Goodhill, G. J. (2004). Influence of lateral connections on the structure of cortical maps. *J. Neurophysiol.* **92,** 2947–2959.

Casseday, J. H., Ehrlich, D., and Covey, E. (1994). Neural tuning for sound duration: Role of inhibitory mechanisms in the inferior colliculus. *Science* **264,** 847–850.

Casseday, J. H., Ehrlich, D., and Covey, E. (2000). Neural measurement of sound duration: Control by excitatory-inhibitory interactions in the inferior colliculus. *J. Neurophysiol.* **84,** 1475–1487.

Cetas, J. S., Price, R. O., Velenovsky, D. S., Sinex, D. G., and McMullen, N. T. (2001). Frequency organization and cellular lamination in the medial geniculate body of the rabbit. *Hearing Res.* **155,** 113–123.

Cetas, J. S., Price, R. O., Crowe, J., Velenovsky, D. S., and McMullen, N. T. (2003). Dendritic orientation and laminar architecture in the rabbit auditory thalamus. *J. Comp. Neurol.* **458,** 307–317.

Cetas, J. S., Price, R. O., Velenovsky, D. S., Crowe, J. J., Sinex, D. G., and McMullen, N. T. (2002). Cell types and response properties of neurons in the ventral division of the medial geniculate body of the rabbit. *J. Comp. Neurol.* **445,** 78–96.

Clarey, J. C., Barone, P., Irons, W. A., Samson, F. K., and Imig, T. J. (1995). Comparison of noise and tone azimuth tuning of neurons in cat primary auditory cortex and medical geniculate body. *J. Neurophysiol.* **74,** 961–980.

Creutzfeldt, O., Hellweg, F. C., and Schreiner, C. (1980). Thalamocortical transformation of responses to complex auditory stimuli. *Exp. Brain Res.* **39,** 87–104.

Davis, K. A., and Young, E. D. (2000). Pharmacological evidence of inhibitory and disinhibitory neuronal circuits in dorsal cochlear nucleus. *J. Neurophysiol.* **83,** 926–940.

Davis, K. A., Ramachandran, R., and May, B. J. (1999). Single-unit responses in the inferior colliculus of decerebrate cats. II. Sensitivity to interaural level differences. *J. Neurophysiol.* **82,** 164–175.

Davis, K. A., Ramachandran, R., and May, B. J. (2003). Auditory processing of spectral cues for sound localization in the inferior colliculus. *J. Assoc. Res. Otolaryngol.* **4,** 148–163.

de Boer, E., and de Jongh, H. R. (1967). Correlation studies applied to the frequency resolution of the cochlea. *J. Aud. Res.* **7,** 209–217.

de Boer, E., and de Jongh, H. R. (1978). On cochlear encoding: Potentialities and limitations of the reverse-correlation technique. *J. Acoust. Soc. Am.* **63,** 115–135.

deCharms, R. C., Blake, D. T., and Merzenich, M. M. (1998). Optimizing sound features for cortical neurons. *Science* **280,** 1439–1443.

Delgutte, B., Joris, P. X., Litovsky, R. Y., and Yin, T. C. (1999). Receptive fields and binaural interactions for virtual-space stimuli in the cat inferior colliculus. *J. Neurophysiol.* **81,** 2833–2851.

Depireux, D. A., Simon, J. Z., Klein, D. J., and Shamma, S. A. (2001). Spectro-temporal response field characterization with dynamic ripples in ferret primary auditory cortex. *J. Neurophysiol.* **85,** 1220–1234.

Eggermont, J. J. (1994). Temporal modulation transfer functions for AM and FM stimuli in cat auditory cortex. Effects of carrier type, modulating waveform and intensity. *Hearing Res.* **74,** 51–66.

Eggermont, J. J. (1999). The magnitude and phase of temporal modulation transfer functions in cat auditory cortex. *J. Neurosci.* **19,** 2780–2788.

Eggermont, J. J., Johannesma, P. M., and Aertsen, A. M. (1983). Reverse-correlation methods in auditory research. *Q. Rev. Biophys.* **16,** 341–414.

Egorova, M., Ehret, G., Vartanian, I., and Esser, K. H. (2001). Frequency response areas of neurons in the mouse inferior colliculus. I. Threshold and tuning characteristics. *Exp. Brain Res.* **140,** 145–161.

Ehret, G., and Merzenich, M. M. (1985). Auditory midbrain responses parallel spectral integration phenomena. *Science* **227,** 1245–1247.

Ehret, G., and Merzenich, M. M. (1988a). Neuronal discharge rate is unsuitable for encoding sound intensity at the inferior-colliculus level. *Hearing Res.* **35,** 1–7.

Ehret, G., and Merzenich, M. M. (1988b). Complex sound analysis (frequency resolution, filtering and spectral integration) by single units of the inferior colliculus of the cat. *Brain Res.* **472,** 139–163.

Ehret, G., and Schreiner, C. E. (1997). Frequency resolution and spectral integration (critical band analysis) in single units of the cat primary auditory cortex. *J. Comp. Physiol. [A]* **181,** 635–650.

Ehret, G., Egorova, M., Hage, S. R., and Muller, B. A. (2003). Spatial map of frequency tuning-curve shapes in the mouse inferior colliculus. *Neuroreport* **14,** 1365–1369.

Escabí, M. A., and Schreiner, C. E. (2002). Nonlinear spectrotemporal sound analysis by neurons in the auditory midbrain. *J. Neurosci.* **22,** 4114–4131.

Escabí, M. A., Miller, L. M., Read, H. L., and Schreiner, C. E. (2003). Naturalistic auditory contrast improves spectrotemporal coding in the cat inferior colliculus. *J. Neurosci.* **23,** 11489–11504.

Evans, E. F., and Palmer, A. R. (1980). Relationship between the dynamic range of cochlear nerve fibers and their spontaneous activity. *Exp. Brain Res.* **40,** 115–118.

Fitzpatrick, D. C., Batra, R., Stanford, T. R., and Kuwada, S. (1997). A neuronal population code for sound localization. *Nature* **388,** 871–874.

Fletcher, H. (1940). Auditory patterns. *Rev. Mod. Phys.* **12,** 47–65.

Fritz, J., Shamma, S., Elhilali, M., and Klein, D. (2003). Rapid task-related plasticity of spectrotemporal receptive fields in primary auditory cortex. *Nat Neurosci* **6,** 1216–1223.

Ghitza, O., and Goldstein, J. L. (1983). JNDs for the spectral envelope parameters in natural speech. *In* "Hearing: Physiological Bases and Psychophysics" (R. Klinke and R. Hartmann, Eds.), pp. 352–359. Springer Verlag, New York.

Gilbert, C. D., and Wiesel, T. N. (1989). Columnar specificity of intrinsic horizontal and corticocortical connections in cat visual cortex. *J. Neurosci.* **9,** 2432–2442.

Greenwood, D. D. (1990). A cochlear frequency-position function for several species—29 years later. *J. Acoust. Soc. Am.* **87,** 2592–2605.

He, J. (2002). OFF responses in the auditory thalamus of the guinea pig. *J. Neurophysiol.* **88,** 2377–2386.

He, J., and Hu, B. (2002). Differential distribution of burst and single-spike responses in auditory thalamus. *J. Neurophysiol.* **88,** 2152–2156.

Heil, P. (1997a). Auditory cortical onset responses revisited. I. First-spike timing. *J. Neurophysiol.* **77,** 2616–2641.

Heil, P. (1997b). Aspects of temporal processing of FM stimuli in primary auditory cortex. *Acta Otolaryngol. Suppl.* **532,** 99–102.

Heil, P. (1997c). Auditory cortical onset responses revisited. II. Response strength. *J. Neurophysiol.* **77,** 2642–2660.

Heil, P., Rajan, R., and Irvine, D. R. F. (1994). Topographic representation of tone intensity along the isofrequency axis of cat primary auditory-cortex. *Hearing Res.* **76,** 188–202.

Henkel, C. K., and Spangler, K. M. (1983). Organization of the efferent projections of the medial superior olivary nucleus in the cat as revealed by HRP and autoradiographic tracing methods. *J. Comp. Neurol.* **221,** 416–428.

Imaizumi, K., Priebe, N. J., Crum, P. A., Bedenbaugh, P. H., Cheung, S. W., and Schreiner, C. E. (2004). Modular functional organization of cat anterior auditory field. *J. Neurophysiol.* **92,** 444–457.

Imig, T. J., and Morel, A. (1985). Tonotopic organization in ventral nucleus of medial geniculate body in the cat. *J. Neurophysiol.* **53,** 309–340.

Imig, T. J., Bibikov, N. G., Poirier, P., and Samson, F. K. (2000). Directionality derived from pinna-cue spectral notches in cat dorsal cochlear nucleus. *J. Neurophysiol.* **83,** 907–925.

Irvine, D. R. (1992). Physiology of the auditory brainstem. *In* "The Mammalian Auditory Pathway: Neurophysiology" (A. N. Popper and R. R. Fay, Eds.), pp. 153–231. Springer, New York.

Jenkins, W. M., and Masterton, R. B. (1982). Sound localization: Effects of unilateral lesions in central auditory system. *J. Neurophysiol.* **47,** 987–1016.

Jenkins, W. M., and Merzenich, M. M. (1984). Role of cat primary auditory cortex for sound-localization behavior. *J. Neurophysiol.* **52,** 819–847.

Jesteadt, W., Bacon, S. P., and Lehman, J. R. (1982). Forward masking as a function of frequency, masker level, and signal delay. *J. Acoust. Soc. Am.* **71,** 950–962.

Johannesma, P., and Aertsen, A. (1982). Statistical and dimensional analysis of the neural representation of the acoustic biotope of the frog. *J. Med. Syst.* **6,** 399–421.

Kanold, P. O., and Young, E. D. (2001). Proprioceptive information from the pinna provides somatosensory input to cat dorsal cochlear nucleus. *J. Neurosci.* **21,** 7848–7858.

Keller, C. H., and Takahashi, T. T. (2000). Representation of temporal features of complex sounds by the discharge patterns of neurons in the owl's inferior colliculus. *J. Neurophysiol.* **84,** 2638–2650.

Klein, D. J., Depireux, D. A., Simon, J. Z., and Shamma, S. A. (2000). Robust spectrotemporal reverse correlation for the auditory system: Optimizing stimulus design. *J. Comput. Neurosci.* **9,** 85–111.

Kowalski, N., Versnel, H., and Shamma, S. A. (1995). Comparison of responses in the anterior and primary auditory fields of the ferret cortex. *J. Neurophysiol.* **73,** 1513–1523.

Kowalski, N., Depireux, D. A., and Shamma, S. A. (1996). Analysis of dynamic spectra in ferret primary auditory cortex. I. Characteristics of single-unit responses to moving ripple spectra. *J. Neurophysiol.* **76,** 3503–3523.

Kuwada, S., Batra, R., Yin, T. C., Oliver, D. L., Haberly, L. B., and Stanford, T. R. (1997). Intracellular recordings in response to monaural and binaural stimulation of neurons in the inferior colliculus of the cat. *J. Neurosci.* **17,** 7565–7581.

Kvale, M. N., and Schreiner, C. E. (2004). Short-term adaptation of auditory receptive fields to dynamic stimuli. *J. Neurophysiol.* **91,** 604–612.

Langner, G. (1997). Neural processing and representation of periodicity pitch. *Acta Otolaryngol. Suppl.* **532,** 68–76.

Langner, G., and Schreiner, C. E. (1988). Periodicity coding in the inferior colliculus of the cat. I. Neuronal mechanisms. *J. Neurophysiol.* **60,** 1799–1822.

Langner, G., Albert, M., and Briede, T. (2002). Temporal and spatial coding of periodicity information in the inferior colliculus of awake chinchilla (Chinchilla laniger). *Hearing Res.* **168,** 110–130.

Le Beau, F. E., Rees, A., and Malmierca, M. S. (1996). Contribution of GABA- and glycine-mediated inhibition to the monaural temporal response properties of neurons in the inferior colliculus. *J. Neurophysiol.* **75,** 902–919.

Liang, L., Lu, T., and Wang, X. (2002). Neural representations of sinusoidal amplitude and frequency modulations in the primary auditory cortex of awake primates. *J. Neurophysiol.* **87,** 2237–2261.

Liberman, M. C. (1982). The cochlear frequency map for the cat: Labeling auditory-nerve fibers of known characteristic frequency. *J. Acoust. Soc. Am.* **72,** 1441–1449.

Linden, J. F., Liu, R. C., Sahani, M., Schreiner, C. E., and Merzenich, M. M. (2003). Spectrotemporal structure of receptive fields in areas AI and AAF of mouse auditory cortex. *J. Neurophysiol.* **90,** 2660–2675.

Luczak, A., Hackett, T. A., Kajikawa, Y., and Laubach, M. (2004). Multivariate receptive field mapping in marmoset auditory cortex. *J. Neurosci. Methods* **136,** 77–85.

Machens, C. K., Wehr, M. S., and Zador, A. M. (2004). Linearity of cortical receptive fields measured with natural sounds. *J. Neurosci.* **24,** 1089–1100.

Malhotra, S., Hall, A. J., and Lomber, S. G. (2004). Cortical control of sound localization in the cat: Unilateral cooling deactivation of 19 cerebral areas. *J. Neurophysiol.* **92,** 1625–1643.

Malmierca, M. S., Rees, A., Le Beau, F. E., and Bjaalie, J. G. (1995). Laminar organization of frequency-defined local axons within and between the inferior colliculi of the guinea pig. *J. Comp. Neurol.* **357,** 124–144.

May, B. J. (2000). Role of the dorsal cochlear nucleus in the sound localization behavior of cats. *Hearing Res.* **148,** 74–87.

McAlpine, D. (2004). Neural sensitivity to periodicity in the inferior colliculus: Evidence for the role of cochlear distortions. *J. Neurophysiol.* **92,** 1295–1311.

Mendelson, J. R., Schreiner, C. E., Sutter, M. L., and Grasse, K. L. (1993). Functional topography of cat primary auditory cortex: Responses to frequency-modulated sweeps. *Exp. Brain Res.* **94,** 65–87.

Merzenich, M. M., and Reid, M. D. (1974). Representation of the cochlea within the inferior colliculus of the cat. *Brain Res.* **77,** 397–415.

Merzenich, M. M., Knight, P. L., and Roth, G. L. (1975). Representation of cochlea within primary auditory cortex in the cat. *J. Neurophysiol.* **38,** 231–249.

Middlebrooks, J. C., and Green, D. M. (1991). Sound localization by human listeners. *Annu. Rev. Psychol.* **42,** 135–159.

Middlebrooks, J. C., Dykes, R. W., and Merzenich, M. M. (1980). Binaural response-specific bands in primary auditory cortex (AI) of the cat: Topographical organization orthogonal to isofrequency contours. *Brain Res.* **181,** 31–48.

Miller, G. A. (1947). Sensitivity to changes in the intensity of white noise and its relation to masking and loudness. *J. Acoust. Soc. Am.* **191,** 609–619.

Miller, L. M., Escabí, M. A., Read, H. L., and Schreiner, C. E. (2001). Functional convergence of response properties in the auditory thalamocortical system. *Neuron* **32,** 151–160.

Miller, L. M., Escabí, M. A., Read, H. L., and Schreiner, C. E. (2002). Spectrotemporal receptive fields in the lemniscal auditory thalamus and cortex. *J. Neurophysiol.* **87,** 516–527.

Nelken, I., and Young, E. D. (1994). Two separate inhibitory mechanisms shape the responses of dorsal cochlear nucleus type IV units to narrowband and wideband stimuli. *J. Neurophysiol.* **71,** 2446–2462.

Nelken, I., and Versnel, H. (2000). Responses to linear and logarithmic frequency-modulated sweeps in ferret primary auditory cortex. *Eur. J. Neurosci.* **12,** 549–562.

Oertel, D., and Young, E. D. (2004). What's a cerebellar circuit doing in the auditory system? *Trends Neurosci.* **27,** 104–110.

Oliver, D. L. (2000). Ascending efferent projections of the superior olivary complex. *Microsc. Res. Tech.* **51,** 355–363.

Oliver, D. L., and Morest, D. K. (1984). The central nucleus of the inferior colliculus in the cat. *J. Comp. Neurol.* **222,** 237–264.

Oliver, D. L., and Shneiderman, A. (1989). An EM study of the dorsal nucleus of the lateral lemniscus: Inhibitory, commissural, synaptic connections between ascending auditory pathways. *J. Neurosci.* **9,** 967–982.

Oliver, D. L., Beckius, G. E., and Shneiderman, A. (1995). Axonal projections from the lateral and medial superior olive to the inferior colliculus of the cat: A study using electron microscopic autoradiography. *J. Comp. Neurol.* **360,** 17–32.

Oliver, D. L., Beckius, G. E., Bishop, D. C., Loftus, W. C., and Batra, R. (2003). Topography of interaural temporal disparity coding in projections of medial superior olive to inferior colliculus. *J. Neurosci.* **23,** 7438–7449.

Orman, S. S., and Phillips, D. P. (1984). Binaural interactions of single neurons in posterior field of cat auditory cortex. *J. Neurophysiol.* **51,** 1028–1039.

Park, T. J., and Pollak, G. D. (1993). GABA shapes sensitivity to interaural intensity disparities in the mustache bat's inferior colliculus: Implications for encoding sound location. *J. Neurosci.* **13,** 2050–2067.

Peruzzi, D., Sivaramakrishnan, S., and Oliver, D. L. (2000). Identification of cell types in brain slices of the inferior colliculus. *NeuroScience* **101,** 403–416.

Peruzzi, D., Bartlett, E., Smith, P. H., and Oliver, D. L. (1997). A monosynaptic GABAergic input from the inferior colliculus to the medial geniculate body in rat. *J. Neurosci.* **17,** 3766–3777.

Phillips, D. P., and Irvine, D. R. (1981). Responses of single neurons in physiologically defined primary auditory cortex (AI) of the cat: Frequency tuning and responses to intensity. *J. Neurophysiol.* **45,** 48–58.

Phillips, D. P., Orman, S. S., Musicant, A. D., and Wilson, G. F. (1985). Neurons in the cat's primary auditory cortex distinguished by their responses to tones and wide-spectrum noise. *Hearing Res.* **18,** 73–86.

Poirier, P., Samson, F. K., and Imig, T. J. (2003). Spectral shape sensitivity contributes to the azimuth tuning of neurons in the cat's inferior colliculus. *J. Neurophysiol.* **89,** 2760–2777.

Pollak, G. D., and Park, T. J. (1993). The effects of GABAergic inhibition on monaural response properties of neurons in the mustache bat's inferior colliculus. *Hearing Res.* **65,** 99–117.

Pollak, G. D., Burger, R. M., and Klug, A. (2003). Dissecting the circuitry of the auditory system. *Trends Neurosci.* **26,** 33–39.

Pollak, G. D., Burger, R. M., Park, T. J., Klug, A., and Bauer, E. E. (2002). Roles of inhibition for transforming binaural properties in the brainstem auditory system. *Hearing Res.* **168,** 60–78.

Poon, P. W., Chen, X., and Hwang, J. C. (1991). Basic determinants for FM responses in the inferior colliculus of rats. *Exp. Brain Res.* **83,** 598–606.

Poon, P. W., Sun, X., Kamada, T., and Jen, P. H. (1990). Frequency and space representation in the inferior colliculus of the FM bat, Eptesicus fuscus. *Exp. Brain Res.* **79,** 83–91.

Populin, L. C., and Yin, T. C. (1998). Behavioral studies of sound localization in the cat. *J. Neurosci.* **18,** 2147–2160.

Portfors, C. V., and Wenstrup, J. J. (2002). Excitatory and facilitatory frequency response areas in the inferior colliculus of the mustached bat. *Hearing Res.* **168,** 131–138.

Qiu, A., Schreiner, C. E., and Escabí, M. A. (2003). Gabor analysis of auditory midbrain receptive fields: Spectro-temporal and binaural composition. *J. Neurophysiol.* **90,** 456–476.

Ramachandran, R., and May, B. J. (2002). Functional segregation of ITD sensitivity in the inferior colliculus of decerebrate cats. *J. Neurophysiol.* **88,** 2251–2261.

Ramachandran, R., Davis, K. A., and May, B. J. (1999). Single-unit responses in the inferior colliculus of decerebrate cats. I. Classification based on frequency response maps. *J. Neurophysiol.* **82,** 152–163.

Ramachandran, R., Davis, K. A., and May, B. J. (2000). Rate representation of tones in noise in the inferior colliculus of decerebrate cats. *J. Assoc. Res. Otolaryngol.* **1,** 144–160.

Read, H. L., Winer, J. A., and Schreiner, C. E. (2001). Modular organization of intrinsic connections associated with spectral tuning in cat auditory cortex. *Proc. Natl. Acad Sci. USA* **98,** 8042–8047.

Read, H. L., Miller, L. M., Escabí, M. A., Schreiner, C. E., and Winer, J. A. (2004). Ventral medial geniculate neucleus contains functionally and anatomically distinct compartments. *Assoc. Res. Otolaryngol. Abs.* **27,** 1457.

Rees, A., and Møller, A. R. (1983). Responses of neurons in the inferior colliculus of the rat to AM and FM tones. *Hearing Res.* **10,** 301–330.

Rees, A., and Møller, A. R. (1987). Stimulus properties influencing the responses of inferior colliculus neurons to amplitude-modulated sounds. *Hearing Res.* **27,** 129–143.

Rees, A., and Palmer, A. R. (1988). Rate-intensity functions and their modification by broadband noise for neurons in the guinea pig inferior colliculus. *J. Acoust. Soc. Am.* **83,** 1488–1498.

Reid, R. C., Soodak, R. E., and Shapley, R. M. (1991). Directional selectivity and spatiotemporal structure of receptive fields of simple cells in cat striate cortex. *J. Neurophysiol.* **66,** 505–529.

Rose, J. E., Greenwood, D. D., Goldberg, J. M., and Hind, J. E. (1963). Some discharge characteristics of single neurons in the inferior colliculus of the cat: I. Tonotopical organization,

relation of spike-counts to tone intensity, and firing patterns of single elements. *J. Neurophysiol.* **26,** 294–320.

Rouiller, E., de Ribaupierre, Y., Morel, A., and de Ribaupierre, F. (1983). Intensity functions of single unit responses to tone in the medial geniculate body of cat. *Hearing Res.* **11,** 235–247.

Rutkowski, R. G., Shackleton, T. M., Schnupp, J. W., Wallace, M. N., and Palmer, A. R. (2002). Spectrotemporal receptive field properties of single units in the primary, dorsocaudal and ventrorostral auditory cortex of the guinea pig. *Audiol. Neurootol.* **7,** 214–227.

Ryugo, D. K., and May, S. K. (1993). The projections of intracellularly labeled auditory nerve fibers to the dorsal cochlear nucleus of cats. *J. Comp. Neurol.* **329,** 20–35.

Saint Marie, R. L., Luo, L., and Ryan, A. F. (1999). Spatial representation of frequency in the rat dorsal nucleus of the lateral lemniscus as revealed by acoustically induced c-fos mRNA expression. *Hearing Res.* **128,** 70–74.

Samson, F. K., Clarey, J. C., Barone, P., and Imig, T. J. (1993). Effects of ear plugging on single-unit azimuth sensitivity in cat primary auditory cortex. I. Evidence for monaural directional cues. *J. Neurophysiol.* **70,** 492–511.

Samson, F. K., Barone, P., Clarey, J. C., and Imig, T. J. (1994). Effects of ear plugging on single-unit azimuth sensitivity in cat primary auditory cortex. II. Azimuth tuning dependent upon binaural stimulation. *J. Neurophysiol.* **71,** 2194–2216.

Samson, F. K., Barone, P., Irons, W. A., Clarey, J. C., Poirier, P., and Imig, T. J. (2000). Directionality derived from differential sensitivity to monaural and binaural cues in the cat's medial geniculate body. *J. Neurophysiol.* **84,** 1330–1345.

Schnupp, J. W., Mrsic-Flogel, T. D., and King, A. J. (2001). Linear processing of spatial cues in primary auditory cortex. *Nature* **414,** 200–204.

Schreiner, C. E., and Langner, G. (1988). Periodicity coding in the inferior colliculus of the cat. II. Topographical organization. *J. Neurophysiol.* **60,** 1823–1840.

Schreiner, C. E., and Urbas, J. V. (1988). Representation of amplitude modulation in the auditory cortex of the cat. II. Comparison between cortical fields. *Hearing Res.* **32,** 49–63.

Schreiner, C. E., and Mendelson, J. R. (1990). Functional topography of cat primary auditory cortex: Distribution of integrated excitation. *J. Neurophysiol.* **64,** 1442–1459.

Schreiner, C. E., and Calhoun, B. M. (1994). Spectral envelope coding in the cat primary auditory cortex. *Aud. Neurosci.* **1,** 39–61.

Schreiner, C. E., and Langner, G. (1997). Laminar fine structure of frequency organization in auditory midbrain. *Nature* **388,** 383–386.

Schreiner, C. E., Mendelson, J. R., and Sutter, M. L. (1992). Functional topography of cat primary auditory cortex: Representation of tone intensity. *Exp. Brain Res.* **92,** 105–122.

Schreiner, C. E., Read, H. L., and Sutter, M. L. (2000). Modular organization of frequency integration in primary auditory cortex. *Annu. Rev. Neurosci.* **23,** 501–529.

Semple, M. N., and Aitkin, L. M. (1979). Representation of sound frequency and laterality by units in central nucleus of cat inferior colliculus. *J. Neurophysiol.* **42,** 1626–1639.

Semple, M. N., and Kitzes, L. M. (1985). Single-unit responses in the inferior colliculus: Different consequences of contralateral and ipsilateral auditory stimulation. *J. Neurophysiol.* **53,** 1467–1482.

Sen, K., Theunissen, F. E., and Doupe, A. J. (2001). Feature analysis of natural sounds in the songbird auditory forebrain. *J. Neurophysiol.* **86,** 1445–1458.

Serviere, J., Webster, W. R., and Calford, M. B. (1984). Isofrequency labeling revealed by a combined [14C]-2-deoxyglucose, electrophysiological, and horseradish peroxidase study of the inferior colliculus of the cat. *J. Comp. Neurol.* **228,** 463–477.

Shamma, S. A., Fleshman, J. W., Wiser, P. R., and Versnel, H. (1993). Organization of response areas in ferret primary auditory cortex. *J. Neurophysiol.* **69,** 367–383.

Shneiderman, A., and Oliver, D. L. (1989). EM autoradiographic study of the projections from the dorsal nucleus of the lateral lemniscus: A possible source of inhibitory inputs to the inferior colliculus. *J. Comp. Neurol.* **286,** 28–47.

Shneiderman, A., Oliver, D. L., and Henkel, C. K. (1988). Connections of the dorsal nucleus of the lateral lemniscus: An inhibitory parallel pathway in the ascending auditory system? *J. Comp. Neurol.* **276,** 188–208.

Singh, N. C., and Theunissen, F. E. (2003). Modulation spectra of natural sounds and ethological theories of auditory processing. *J. Acoust. Soc. Am.* **114,** 3394–3411.

Smith, A. L., Parsons, C. H., Lanyon, R. G., Bizley, J. K., Akerman, C. J., Baker, G. E., Dempster, A. C., Thompson, I. D., and King, A. J. (2004). An investigation of the role of auditory cortex in sound localization using muscimol-releasing Elvax. *Eur. J. Neurosci.* **19,** 3059–3072.

Snyder, R. L., Leake, P. A., and Hradek, G. T. (1997). Quantitative analysis of spiral ganglion projections to the cat cochlear nucleus. *J. Comp. Neurol.* **379,** 133–149.

Spirou, G. A., May, B. J., Wright, D. D., and Ryugo, D. K. (1993). Frequency organization of the dorsal cochlear nucleus in cats. *J. Comp. Neurol.* **329,** 36–52.

Spirou, G. A., Davis, K. A., Nelken, I., and Young, E. D. (1999). Spectral integration by type II interneurons in dorsal cochlear nucleus. *J. Neurophysiol.* **82,** 648–663.

Stevens, S. S. (1957). On the psychophysical laws. *Psychol. Rev.* **64,** 153–181.

Stiebler, I., and Ehret, G. (1985). Inferior colliculus of the house mouse. I. A quantitative study of tonotopic organization, frequency representation, and tone-threshold distribution. *J. Comp. Neurol.* **238,** 65–76.

Sutter, M. L., and Schreiner, C. E. (1991). Physiology and topography of neurons with multipeaked tuning curves in cat primary auditory cortex. *J. Neurophysiol.* **65,** 1207–1226.

Theunissen, F. E., Sen, K., and Doupe, A. J. (2000). Spectral-temporal receptive fields of nonlinear auditory neurons obtained using natural sounds. *J. Neurosci.* **20,** 2315–2331.

Thompson, A. M., and Schofield, B. R. (2000). Afferent projections of the superior olivary complex. *Microsc. Res. Tech.* **51,** 330–354.

Tollin, D. J. (2003). The lateral superior olive: A functional role in sound source localization. *Neuroscientist* **9,** 127–143.

Tollin, D. J., and Yin, T. C. (2003). Spectral cues explain illusory elevation effects with stereo sounds in cats. *J. Neurophysiol.* **90,** 525–530.

Valentine, P. A., and Eggermont, J. J. (2004). Stimulus dependence of spectro-temporal receptive fields in cat primary auditory cortex. *Hearing Res.* **196,** 119–133.

Velenovsky, D. S., Cetas, J. S., Price, R. O., Sinex, D. G., and McMullen, N. T. (2003). Functional subregions in primary auditory cortex defined by thalamocortical terminal arbors: An electrophysiological and anterograde labeling study. *J. Neurosci.* **23,** 308–316.

Versnel, H., and Shamma, S. A. (1998). Spectral-ripple representation of steady-state vowels in primary auditory cortex. *J. Acoust. Soc. Am.* **103,** 2502–2514.

Versnel, H., Kowalski, N., and Shamma, S. (1995). Ripple analysis in ferret primary auditory cortex. III. Topographic distribution of ripple response parameters. *Aud. Neurosci.* **1,** 271–285.

Wehr, M., and Zador, A. M. (2003). Balanced inhibition underlies tuning and sharpens spike timing in auditory cortex. *Nature* **426,** 442–446.

Winer, J. A., Saint Marie, R. L., Larue, D. T., and Oliver, D. L. (1996). GABAergic feedforward projections from the inferior colliculus to the medial geniculate body. *Proc. Natl. Acad. Sci. USA* **93,** 8005–8010.

Xu, L., Furukawa, S., and Middlebrooks, J. C. (1998). Sensitivity to sound-source elevation in nontonotopic auditory cortex. *J. Neurophysiol.* **80,** 882–894.

Xu, L., Furukawa, S., and Middlebrooks, J. C. (1999). Auditory cortical responses in the cat to sounds that produce spatial illusions. *Nature* **399,** 688–691.

Yeshurun, Y., Wollberg, Z., and Dyn, N. (1989). Prediction of linear and non-linear responses of MGB neurons by system identification methods. *Bull. Math. Biol.* **51,** 337–346.

Young, E. D., Spirou, G. A., Rice, J. J., and Voigt, H. F. (1992). Neural organization and responses to complex stimuli in the dorsal cochlear nucleus. *Philos. Trans. R. Soc. Lond. B. Biol. Sci.* **336,** 407–413.

Yu, J. J., and Young, E. D. (2000). Linear and nonlinear pathways of spectral information transmission in the cochlear nucleus. *Proc. Natl. Acad. Sci. USA* **97,** 11780–11786.

Zhang, L. I., Tan, A. Y., Schreiner, C. E., and Merzenich, M. M. (2003). Topography and synaptic shaping of direction selectivity in primary auditory cortex. *Nature* **424,** 201–205.

Zwicker, E., Flottorp, G., and Stevens, S. S. (1957). Critical band width in loudness summation. *J. Acoust. Soc. Am.* **29,** 548–557.